Development of Procedure for Low-Constraint Toughness Testing Using a Single-Specimen Technique

Final Report 277-T-03

For Project

Weld Design, Testing, and Assessment Procedures for High Strength Pipelines

Prepared for the

Design, Materials, and Construction Technical Committee of
Pipeline Research Council International, Inc.
Project MATH-1 Catalog No. L5XXXX

and

U.S. Department of Transportation
Pipeline and Hazardous Materials Safety Administration
Office of Pipeline Safety
Agreement Number DTPH56-07-T-000005

Prepared by

G. Shen, J.A. Gianetto and W.R. Tyson
CANMET Materials Technology Laboratory

September 2011

This research was funded in part under the Department of Transportation, Pipeline and Hazardous Materials Safety Administration's Pipeline Safety Research and Development Program. The views and conclusions contained in this document are those of the authors and should not be interpreted as representing the official policies, either expressed or implied, of the Pipeline and Hazardous Materials Safety Administration, or the U.S. Government.

CANMET Materials Technology Laboratory

Development of Procedure for Low-Constraint Toughness Testing Using a Single-Specimen Technique

G. Shen, J.A. Gianetto and W.R. Tyson

CANMET Materials Technology Laboratory
Minerals and Metals Sector, Natural Resources Canada
183 Longwood Road South, Hamilton, ON, Canada, L8P 0A5

CANMET Report No. 2008-18(TR)

September 2011

DISCLAIMER

Natural Resources Canada makes no representations or warranties respecting the contents of this report, either expressed or implied, arising by law or otherwise, including but not limited to implied warranties or conditions of merchantability or fitness for a particular purpose.

Catalog No. L5XXXX

Development of Procedure for Low-Constraint Toughness Testing Using a Single-Specimen Technique

Final Report 277-T-03

For Project

Weld Design, Testing, and Assessment Procedures for High Strength Pipelines

Prepared for the

Design, Materials, and Construction Technical Committee of
Pipeline Research Council International, Inc.
Project MATH-1 Catalog No. L5XXXX

and

U.S. Department of Transportation
Pipeline and Hazardous Materials Safety Administration
Office of Pipeline Safety
Agreement Number DTPH56-07-T-000005

Prepared by

G. Shen, J.A. Gianetto and W.R. Tyson
CANMET Materials Technology Laboratory

September 2011

Version	Date of Last Revision	Date of Uploading	Comments
1	November 2010	8 April 2011	
Fianl	September 2010	September 2010	

This report is furnished to Pipeline Research Council International, Inc. (PRCI) under the terms of PRCI contract [277-PR-348-074512] between PRCI and the MATH-1 contractors:

- Electricore (prime contractor),
- Center for Reliable Energy Systems, CANMET, NIST, and The Lincoln Electric Company (sub-contractors).

The contents of this report are published as received from the MATH-1 contractor and subcontractors. The opinions, findings, and conclusions expressed in the report are those of the authors and not necessarily those of PRCI, its member companies, or their representatives. Publication and dissemination of this report by PRCI should not be considered an endorsement by PRCI of the MATH-1 contractor and subcontractors, or the accuracy or validity of any opinions, findings, or conclusions expressed herein.

In publishing this report, PRCI and the MATH-1 contractors make no warranty or representation, expressed or implied, with respect to the accuracy, completeness, usefulness, or fitness for purpose of the information contained herein, or that the use of any information, method, process, or apparatus disclosed in this report may not infringe on privately owned rights. PRCI and the MATH-1 contractors assume no liability with respect to the use of, or for damages resulting from the use of, any information, method, process, or apparatus disclosed in this report. By accepting the report and utilizing it, you agree to waive any and all claims you may have, resulting from your voluntary use of the report, against PRCI and the MATH-1 contractors.

Pipeline Research Council International Catalog No. L5XXXX

PRCI Reports are Published by Technical Toolboxes, Inc.

3801 Kirby Drive, Suite 520
Houston, Texas 77098
Tel: 713-630-0505
Fax: 713-630-0560
Email: info@ttoolboxes.com

PROJECT PARTICIPANTS

PROJECT TEAM MEMBER	COMPANY AFFILIATION	PROJECT TEAM MEMBER	COMPANY AFFILIATION
Arti Bhatia	Alliance	Jim Costain	GE
Jennifer Klementis	Alliance	Gilmar Batista	Petrobras
Roger Haycraft	Boardwalk	Marcy Saturno de Menezez	Petrobras
David Horsley	BP	Dave Aguiar	PG&E
Mark Hudson	BP	Ken Lorang	PRCI
Ron Shockley	Chevron	Maslat Al-Waranbi	Saudi Aramco
Sam Mishael	Chevron	Paul Lee	SoCalGas
David Wilson	ConocoPhillips	Alan Lambeth	Spectra
Satish Kulkarni	El Paso	Robert Turner	Stupp
Art Meyer	Enbridge	Gilles Richard	TAMSA
Bill Forbes	Enbridge	Noe Mota Solis	TAMSA
Scott Ironside	Enbridge	Philippe Darcis	TAMSA
Sean Keane	Enbridge	Dave Taylor	TransCanada
Laurie Collins	Evraz	Joe Zhou	TransCanada
David de Miranda	Gassco	Jason Skow	TransGas
Adriaan den Herder	Gasunie	Ernesto Cisneros	Tuberia Laguna
Jeff Stetson	GE	Vivek Kashyap	Welpsun
		Chris Brown	Williams

CORE RESEARCH TEAM	
RESEARCHER	**COMPANY AFFILIATION**
Yaoshan Chen	Center for Reliable Energy Systems
Yong-Yi Wang	Center for Reliable Energy Systems
Ming Liu	Center for Reliable Energy Systems
Dave Fink	Lincoln Electric Company
Marie Quintana	Lincoln Electric Company
Vaidyanath Rajan	Lincoln Electric Company
Joe Daniel	Lincoln Electric Company
Radhika Panday	Lincoln Electric Company
James Gianetto	CANMET Materials Technology Laboratory
John Bowker	CANMET Materials Technology Laboratory
Bill Tyson	CANMET Materials Technology Laboratory
Guowu Shen	CANMET Materials Technology Laboratory
Dong Park	CANMET Materials Technology Laboratory
Timothy Weeks	National Institute of Standards and Technology
Mark Richards	National Institute of Standards and Technology
Dave McColskey	National Institute of Standards and Technology
Enrico Lucon	National Institute of Standards and Technology
John Hammond	Consultant Metallurgist & Welding Engineer

This Page Intentionally Left Blank

FINAL REPORT STRUCTURE

Focus Area 1 - Update of Weld Design, Testing, and Assessment Procedures for High Strength Pipelines		
Report #	**Description**	**Lead Authors**
277-T-01	Background of Linepipe Specifications	CRES/CANMET
277-T-02	Background of All-Weld Metal Tensile Test Protocol	CANMET/Lincoln
277-T-03	Development of Procedure for Low-Constraint Toughness Testing Using a Single-Specimen Technique	CANMET/CRES
277-T-04	Summary of Publications: Single-Edge Notched Tension SE(T) Tests	CANMET
277-T-05	Small Scale Tensile, Charpy V-Notch, and Fracture Toughness Tests	CANMET/NIST
277-T-06	Small Scale Low Constraint Fracture Toughness Test Results	CANMET/NIST
277-T-07	Small Scale Low Constraint Fracture Toughness Test Discussion and Analysis	CANMET/NIST
277-T-08	Summary of Mechanical Properties	CANMET
277-T-09	Curved Wide Plate Tests	NIST/CRES
277-T-10	Weld Strength Mismatch Requirements	CRES/CANMET
277-T-11	Curved Wide Plate Test Results and Transferability of Test Specimens	CRES/CANMET
277-S-01	Summary Report 277 Weld Design, Testing, and Assessment Procedures for High Strength Pipelines	CRES

Focus Area 2 - Development of Optimized Welding Solutions for X100 Linepipe Steel		
Report #	**Description**	**Lead Authors**
278-T-01	State of The Art Review	Lincoln
278-T-02	Material Selection, Welding and Weld Monitoring	Lincoln/CANMET
278-T-03	Microstructure and Hardness Characterization of Girth Welds	CANMET/Lincoln
278-T-04	Microstructure and Properties of Simulated Weld Metals	CANMET/Lincoln
278-T-05	Microstructure and Properties of Simulated Heat Affected Zones	CANMET/Lincoln
278-T-06	Essential Welding Variables	Lincoln/CANMET
278-T-07	Thermal Model for Welding Simulations	CRES/CANMET
278-T-08	Microstructure Model for Welding Simulations	CRES/CANMET
278-T-09	Application to Other Processes	Lincoln/CANMET
278-S-01	Summary Report 278 Development of Optimized Welding Solutions for X100 Line Pipe Steel	Lincoln

EXECUTIVE SUMMARY

This work was performed for specific application to surface circumferential cracks in pipe under strain-based design, for which the best constraint matching has been found to occur for clamped single-edge tension (SE(T)) specimens with H/W=10. For this geometry, a test procedure similar to that of ASTM E1820-06 for single-edge bend (SE(B)) and compact tension (C(T)) specimens was developed for J-resistance tests using a single-specimen technique. All the equations used in the procedure, including those for evaluation of J-integrals from the area under load/plastic crack mouth opening displacement (CMOD) curves, and evaluation of crack length from unloading compliance including rotation correction, were developed using finite element analysis (FEA) with a range of crack depths, focusing on a/W= 0.2 to 0.5 which is of most practical interest. The present procedure is compared with that of E1820 for SE(B) testing regarding evaluation of J-integral with crack growth correction, crack length evaluation, and correction of compliance for rotation. Some details of the tests, such as load used for initial crack size estimation, and selection of side-groove depth for the SE(T) specimens, are also specified and compared with that for SE(B) specimens. The initial and final crack lengths evaluated using the compliance technique are compared with those from the optical nine-point technique on broken specimens. J-integral resistance curves measured using clamped SE(T) specimens and conventional SE(B) specimens, including plain-sided and side-grooved with shallow and deep cracks for the same high strength pipe steel base metal are reported and compared.

TABLE OF CONTENTS

		Page
Executive Summary		viii
Table of Contents		ix
List of Figures		x
List of Tables		xi
Terminology		xii
1	Introduction	1
2	Development of Test procedure	2
2.1	Scope of the Test	2
2.2	Design of Specimens and wedge grip	2
2.3	Notch and Precracking	4
2.4	Measurement of Initial Crack Length and Unload/Reload Range	5
2.5	Revised a_{oq}	5
2.6	Report	6
3	Development of Equations for J-Resistance Test	6
3.1	equations for J Calculation for Resistance Curve Test Method	6
3.2	Finite Element Model	6
3.3	Equations for Stress Intensity Factors	9
3.4	Equations for Elastic CMOD Compliance	10
3.5	Rotation Correction for Unloading Compliance of Clamped SE(T) Specimens	13
3.6	Evaluation of Factor η_{CMOD}	15
3.7	J Evaluation for Growing Crack	17
4	EXPERIMENTS	19
4.1	Materials and Specimens	19
4.2	J-R Tests Using Clamped SE(T) Specimens	20
4.3	J-R Tests Using SE(B) Specimens	25
4.4	Comparison of J-R Curves Measured Using SE(T) and SE(B) Specimens	27
5	Summary and Conclusions	28
6	Acknowledgments	30
7	References	30

LIST OF FIGURES

Figure 1. Drawing of SE(T) specimen. 3
Figure 2. SE(T) specimen and wedge grip. 3
Figure 3. Broken SE(T) specimen with 10% side-groove on each side, a/W=0.25. 4
Figure 4. Broken SE(T) specimen with 5% side-groove On each side, A/W=0.25. 4
Figure 5. Broken SE(T) specimen with 5% side-groove on each side, a/W=0.5. 5
Figure 6. 2-D FEA mesh for clamped SE(T) specimen. 8
Figure 7. 3-D FEA mesh for clamped SE(T) specimen. 8
Figure 8. 3-D FEA mesh for clamped SE(T) specimen with side-groove. 9
Figure 9. Geometry factor G for clamped SE(T) specimen, H/W=10. 10
Figure 10. BCE vs a/W for clamped SE(T) and SE(B) specimens (plane stress). 12
Figure 11. CMOD compliance from 3-D FEA and 2-D equations. 13
Figure 12. Rotation correction coefficients as functions of load for clamped SE(T) specimens (a/W=0.5). 14
Figure 13. Rotation correction coefficients as functions of load for clamped SE(T) specimens (a/W=0.2). 15
Figure 14. Slope of straight line $J_{P(I)}$, $A_{PLCMOD(I)}$/ Bb for deep crack (a/W=0.5). 15
Figure 15. Slope of straight line $J_{P(I)}$, $A_{PLCMOD(I)}$/ Bb for shallow crack (a/W=0.2). 16
Figure 16. Parameter η_{CMOD} as a function of a/W for various N. 16
Figure 17: Comparison of ηCMOD factors. 17
Figure 18. Factor η_{LLD} as a function of a/W for clamped SE(T) specimens, H/W=10. 18
Figure 19. γ_{LLD} as a function of a/W. 19
Figure 20. Stress-strain curves of X100 steel pipe in longitudinal direction (parallel to the pipe axis). 20
Figure 21. P-CMOD curves of clamped SE(T) specimens, X100 steel. 21
Figure 22. Change of unloading compliance during loading-unloading sequence. 22
Figure 23. J-R curves for deeply-cracked SE(T) specimens, crack length without rotation correction (PS-plain-sided, SG-side-grooved). 22
Figure 24. J-R curves for deeply-cracked SE(T) specimens, crack length with rotation correction (PS-plain-sided, SG-side-grooved). 23
Figure 25. J-R curves for shallow-cracked SE(T) specimens, crack length without rotation correction (PS: plain-sided, SG: side-grooved). 23
Figure 26. J-R curves for shallow-cracked SE(T) specimens, crack length with rotation correction (PS: plain-sided, SG: side-grooved) 24
Figure 27. Effect of γ on J-Integral evaluation. 24
Figure 28. Crack length for clamped SE(T) specimens, a_o, a_f-initial and final crack lengths; PS, SG-plain sided and side-grooved specimens. 25
Figure 29. J-R curves for deeply-cracked (a/W=0.5) SE(B) specimens, PS: plain-sided, SG: side-grooved. 26
Figure 30. J-R curves for shallow-cracked (a/W=0.5) SE(B) specimens, PS: plain-sided, SG: side-grooved. 26
Figure 31. J-R curves measured using SE(T) and SE(B) specimens, a/W=0.5. 27
Figure 32. J-R curves measured using SE(T) and SE(B) specimens, a/W=0.25 28

LIST OF TABLES

Table 1. FEA models used in the present study 7
Table 2. Coefficients t_i in Eqn. (7) for H/W=10 and $0.05 \leq a/W \leq 0.95$ 10
Table 3. CMOD compliance for SE(T) specimen, H/W=10. 11
Table 4. Coefficients r_j in Eqn. (10) for H/W= 10 11
Table 5. Coefficients ϕ_i in Eqn. (5) 17
Table 6. Coefficients ψ_i in Eqn. (16) for H/W=10 and $0.1 \leq a/W \leq 0.7$ 18
Table 7. Tensile properties 19

TERMINOLOGY

a	crack size (length)
a_o	original crack size (length)
A_{pl}	area under the load versus plastic crack mouth opening displacement (CMOD)
A_2	constraint parameter
b	remaining ligament (=W-a)
b_o	original ligament (=W-a_o)
B	specimen thickness
B_e	effective thickness for side-grooved specimen (=B-(B-B_N)^2/B)
B_N	specimen net thickness
C_{CMOD}	CMOD compliance, the ratio of CMOD increment to load increment (=$\Delta v/\Delta P$)
C_i	measured CMOD compliance at the i_{th} unloading
$C_{c(i)}$	measured CMOD compliance at the i_{th} unloading in the undeformed configuration
E	modulus of elasticity
E'	= E for plane stress, $E/(1-\nu^2)$ for plane strain
F_r	= (C_i / $C_{c(i)}$) rotation correction factor
G	geometry factor of SE(T) specimen
H	specimen span between two grips
J	J-integral
J_c	J-integral at onset of unstable brittle crack extension after less than 0.2 mm of crack growth
J_u	J-integral at onset of unstable brittle crack extension after at least 0.2 mm of crack growth
J_m	J-integral at maximum load
K	stress intensity factor
N	strain hardening exponent
P	load
P_Y	= $B_N(W-a)\sigma_Y$ for SE(T) specimen
Q	constraint parameter
S	(= 4W) specimen span for SE(B) specimen
v	CMOD
v_{pl}	plastic part of CMOD
W	specimen width
υ	Poisson's ratio
σ	= (P/WB) nominal stress applied on the plate
σ	stress (= P/(BW))
σ_{YS}	0.2% offset yield strength
σ_{TS}	ultimate tensile strength
σ_Y	effective yield strength = (σ_{YS} + σ_{TS})/2
η_{CMOD}	η factor in J-integral –area of load/plastic CMOD curve
γ	crack growth factor in J-integral evaluation
Δa	crack extension
Δv	CMOD increment
ΔP	load increment

1 INTRODUCTION

Pipelines from remote frontier regions are increasingly required to have adequate resistance to large deformations such as that caused by ground movement. In response to this, "strain-based design" has been developed to enable assessment of imperfections at applied strains beyond yield. In addition, it is proposed to take advantage of the increased apparent toughness of pipe under low constraint, such as girth weld imperfections under axial tension, compared with the high-constraint toughness measured in conventional tests such as ASTM E1290 [1]. Application of low-constraint testing has been advantageously applied in assessment of toughness for offshore pipeline projects.

Also in the pipeline industry, demands on new pipeline projects include low design temperatures as well as high strain capacity. At the same time, increased strength is specified, which increases the level of required toughness. These factors make it increasingly important to assure weldment toughness, in particular to ensure that the failure mode remains ductile. It is well known that brittle cleavage is especially sensitive to constraint, and the availability of a toughness test that would reproduce field conditions would enable more rational development and acceptance of candidate welds and, in particular, enable more appropriate testing of weld heat-affected zones.

Recently, a substantial amount of research has been performed to assess the fracture toughness of pipes with low constraint; specimens such as shallow-cracked single-edge bend and tension (SE(B) and SE(T)), either pin-loaded or clamped, have been used. The related work on J-resistance measurement includes work of CANMET-MTL [2], where single-specimen technique on shallow SE(B) and clamped SE(T) specimens was used; the guideline in DNV-RP-F108 [3], where multiple-specimen technique was used on SE(T) specimens; also the work by Silva, Cravero and Ruggieri [4], where pin-loaded SE(T) specimens were used.

Previous studies at CANMET-MTL have involved the development of methods to perform toughness tests by using single edge specimens in tension and bending, and this work has demonstrated that the apparent toughness as measured by the J-integral at a fixed amount of crack growth is indeed higher under low constraint as quantified, for example, by low values of the constraint parameter Q [2]. However, this work has not yet been generalized to form a guideline to enable standardized testing. The goal of the present study is to develop a low-constraint toughness test procedure based on single-edge tension (SE(T)) that will be suitable for standardization.

This report will show the development of procedure and equations for J-resistance of SE(T) tests utilizing a single-specimen technique. The procedure includes pre-test specimen design including selection of length to width ratio, crack depth, as well as the design of side groove geometry. Information related to fatigue crack preparation, loading-unloading schedule (such as defining the load for initial crack measurement and percentage of unloading in loading-unload sequence) and post-test analysis and reporting of initial crack length. The equations used in the procedure include those for evaluation of J-integrals from the area under load/plastic crack mouth opening displacement (CMOD) curves, and evaluation of crack length from unloading

compliance, including rotation correction. The resulting procedure and equations will be compared with those in the literature and in ASTM standard E1820 (for SE(B) testing). Finally, J-resistance results will be reported for an X-100 steel pipe tested using standard SE(B) testing following the methods in ASTM E1820-06 [5] and the newly-developed procedure for clamped SE(T) specimens.

2 DEVELOPMENT OF TEST PROCEDURE

2.1 SCOPE OF THE TEST

The goal of this test is to measure the J-integral fracture toughness and the extent of crack growth using a single-specimen technique on a low constraint specimen. The specimen geometry and loading mode is designed to produce a level of crack-tip constraint in the test that is similar to the constraint experienced in service, specifically surface circumferential crack-like imperfections in pipe under strain based design. The test is intended to be used for structural steels.

For the above goal, a fatigue-pre-cracked specimen will be continuously loaded. Crack extension may occur by ductile tearing, or by unstable brittle crack extension. In the latter case, the value of J will be recorded as either J_c, or as J_u if the brittle extension is preceded by at least 0.2 mm of ductile growth. The value of J at maximum load is recorded as J_m if there has been no prior brittle cracking. If crack extension occurs by stable ductile tearing, a J-R "resistance curve" from measured data will be constructed.

2.2 DESIGN OF SPECIMENS AND WEDGE GRIP

To produce a level of crack-tip constraint in the test that is similar to the constraint experienced in service, stress fields and constraint parameters (Q and A_2) of circumferentially-cracked high strength pipe in displacement-controlled tension were compared with those of small-scale single-edge notched specimens tested in tension (SE(T)) and bending (SE(B)). The factors affecting transferability of fracture toughness (J-resistance) data from small-scale laboratory tests to cracked high strength pipe were investigated. The investigation is written in a separate publication [6].

In that publication [6], it is found that the crack-tip stress field is of similar form for a circumferential crack in a pipe and a SE(T) test specimen, while for a SE(B) specimen there is a significant gradient in the crack-tip stress field. Hence, the fracture toughness can be characterized by only two parameters (J and Q or J and A_2) for tension-loaded pipe and SE(T) tests, but for SE(B) tests one more parameter is needed to describe the bending term.

In that publication [6], it is also concluded that the constraint in a SE(T) test with ratio of span between load points to width H/W=10 provides a reasonable match to that of a circumferential crack in a pipe subjected to tensile loading. Fixed grip loading was selected based on the following two considerations: i) clamped specimen is simpler to make compared with the pin-

loaded specimen; ii) clamped specimen has restricted rotation that avoids effect of large rotation on compliance.

As shown in Figure 1, the SE(T) specimen is clamped at both ends to impose "fixed-grip" loading with a "daylight" between the load points of H=10W.

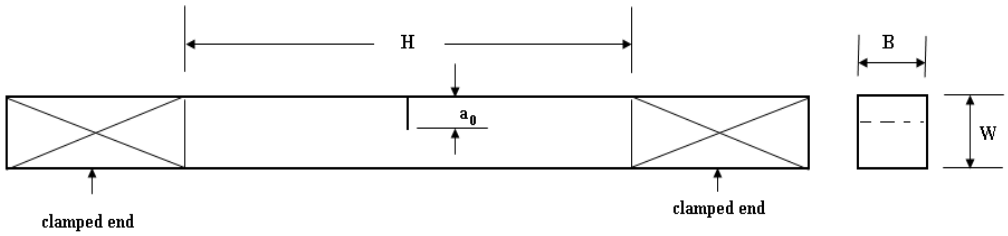

Figure 1. Drawing of SE(T) specimen.

The test can be conducted using a universal test frame, with ancillary equipment for cooling the specimen if required. It should be noted that the load capacity can be significantly higher than that required for bend tests. For an uncracked B×B specimen, the collapse load is $\sigma_Y B^2$ in tension but only $\sigma_Y B^2/4$ in bending (with the usual span of S=4W).

Apparatus is required for measurement of load and crack-mouth opening displacement as described in E 1820 for SE(B) specimens. A SE(T) specimen clamped in an Instron universal testing machine is shown in Figure 2.

Figure 2. SE(T) specimen and wedge grip.

2.3 NOTCH AND PRECRACKING

The notch should be machined following the procedures described for SE(B) specimens in ASTM E1820, Annex A. For simplicity, all specimens can be pre-cracked in three-point bending fatigue following the requirements described in ASTM E1820.2.4.

Side grooves are recommended to promote straight-fronted crack growth. According to E1820, the angle of the side groove should be less than 90°, and the root radius 0.5 ± 0.2 mm. A total reduction of 0.2B and 0.1B were tested for shallow and deep cracked SE(T) specimens. For a shallow crack (a/W=0.25), it was found that excessive crack extension occurred at the edge of the specimen (Figure 3) with a total reduction of 0.2B (0.1B on each side). A total reduction of 0.10B (half that recommended for bend testing) was used initially both for shallow (a/W=0.25, Figure 4) and deep (a/W=0.5, Figure 5) cracks. However, this may not be sufficient to provide plane strain constraint and a SG depth of 15% (7.5% on each side) is now recommended. Precracking is performed prior to side-grooving. The root of the side groove is located along the specimen centerline.

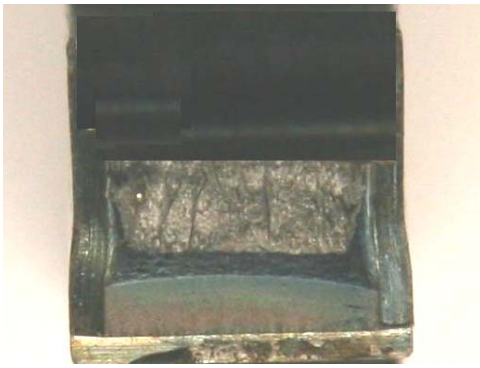

Figure 3. Broken SE(T) specimen with 10% side-groove on each side, a/W=0.25.

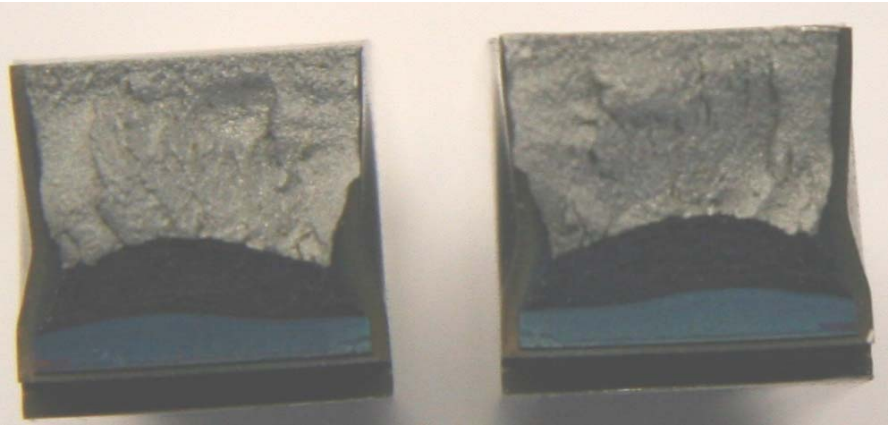

Figure 4. Broken SE(T) specimen with 5% side-groove On each side, A/W=0.25.

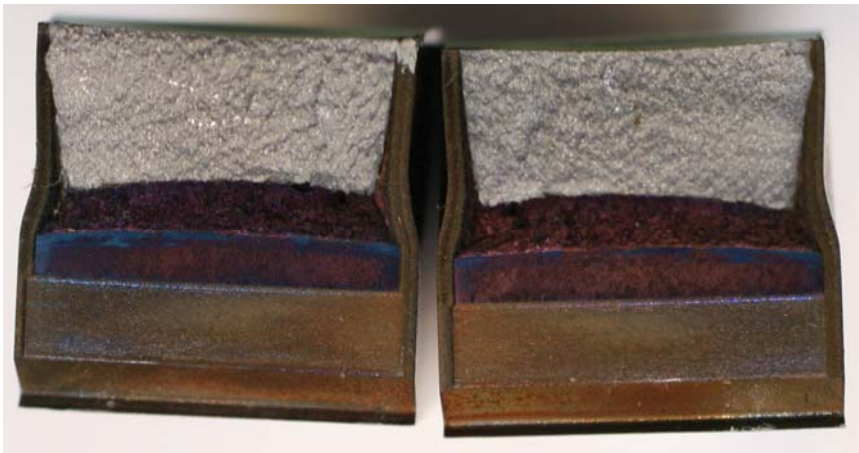

Figure 5. Broken SE(T) specimen with 5% side-groove on each side, a/W=0.5.

2.4 MEASUREMENT OF INITIAL CRACK LENGTH AND UNLOAD/RELOAD RANGE

In J-R tests using a single-specimen technique, unloading compliance is recommended for measurement of the crack length. Measurement of the original crack length, a_o, is usually done by three unloading/reloading sequences. In E1820, the maximum load used for measurement of a_o for a SE(B) specimen is 0.5 to 1.0 times the maximum precracking force ($P_m=0.5Bb_o^2\sigma_Y/S$), that is about 0.25 to 0.5 times the collapse load of a SE(B) specimen. Similarly, for clamped SE(T) specimens, we have used three unloading/ reloading sequences in the load range from 0.25 to 0.5 P_Y ($P_Y=B_N(W-a)\sigma_Y$) for a_o measurement. Equations relating compliance to crack depth are developed in a later section. During the test, unload/reload cycles for compliance measurement are repeated at each point i. It is recommended to use 25% of the current load for a SE(T) specimen as the range of unload/reload for crack extension measurement. This is in the low range of that recommended for SE(B) specimens in E1820 (should not exceed either 50% of P_m or 50% of the current force whichever is smaller). Test results show that the hysteresis loop can be reduced by using a low range of unloading load change.

2.5 REVISED a_{oq}

As done in E 1820, after the test, all J_i and a_i pairs determined before the specimen reached maximum load are identified. The same as required by ASTM E1820, the number of these pairs shall be ≥ 8. This set of data points is used to calculate a revised a_{oq} using the following equation:

$$a = a_{oq} + J/(2\sigma_Y) + BJ^2 + CJ^3 \qquad (1)$$

The coefficients of this equation are found using a least-squares fitting procedure. The revised a_{oq} is then used to estimate values of $\Delta a_i = a_i - a_{oq}$.

After completion of the test, the specimen is heat tinted at about 300°C for 30 min and then broken open. The nine-point technique described in ASTM E1820 is used to measure the crack length for comparison with that from unloading compliance.

2.6 REPORT

The results of the test should be reported in the form of a spreadsheet with original data of load and CMOD, and calculations of J and a. The summary report should include, at a minimum: material; specimen dimensions including side grooving; initial crack length from Eqn. (1); initial and final crack length measured on the fracture surface using the nine-point average technique; and J_c, J_u, J_m as appropriate. The results of the calculations should be shown as a resistance curve, J vs. Δa.

3 DEVELOPMENT OF EQUATIONS FOR J-RESISTANCE TEST

3.1 EQUATIONS FOR J CALCULATION FOR RESISTANCE CURVE TEST METHOD

In the present study, the format for J evaluation in the resistance curve test method recommended in ASTM E1820-06 for the SE(B) specimen geometry (A1.11 and A1.12 [5]) is used for SE(T) specimens, with modification for crack growth. In the equations, J is calculated at point i at current values of crack length $a_{(i)}$, CMOD $v_{(i)}$, and load $P_{(i)}$ as follows:

$$J_{(i)} = \frac{\left((K_{(i)})^2\left(1-\nu^2\right)\right)}{E} + J_{pl(i)} \tag{2}$$

The value of the plastic part of the J integral $J_{pl(i)}$ is given by

$$J_{pl(i)} = \left[J_{pl(i-1)} + \left(\frac{\eta_{CMOD(i-1)}}{b_{(i-1)}}\right)\left(\frac{A_{pl(i)} - A_{pl(i-1)}}{B_N}\right)\right]\left[1 - \frac{\gamma_{LLD}(i-1)\left(a_{(i)} - a_{(i-1)}\right)}{b_{(i-1)}}\right] \tag{3}$$

where the equations for evaluating intensity factors K, parameters η_{CMOD} and γ_{LLD} will be developed using FEA. The current crack length $a_{(i)}$ will be evaluated by the unloading compliance technique. An equation relating crack length and elastic compliance including rotation correction was also developed by FEA.

3.2 FINITE ELEMENT MODEL

FEA was used in the present study to develop equations for evaluation of stress intensity factors as a function of load and crack depth, J-integrals as a function of the area under load/plastic crack mouth opening displacement (CMOD) curves, and crack length as a function of unloading compliance including rotation correction. The calculations were generally conducted by using a 2-D plane strain assumption; a 3-D FEA model was used to test the accuracy of using equations developed using a 2-D model for a 3-D specimen and to find an equivalent thickness B_e for specimens with side-grooves. The details of the FEA models for these calculations are listed in Table 1.

For elastic-plastic material, tensile properties were described using an elastic-power law plastic expression for use in finite element analysis:

$$\begin{aligned} \varepsilon &= \frac{\sigma}{E} && for \quad \sigma \leq \sigma_{YS} \\ \varepsilon &= \frac{\sigma_{YS}}{E}\left(\frac{\sigma}{\sigma_{YS}}\right)^{N} && for \quad \sigma > \sigma_{YS} \end{aligned} \tag{4}$$

Table 1. FEA models used in the present study

Parameters for evaluation	Material model	Deformation	Crack-tip shape
Stress intensity factors	Elastic	-	Sharp (R=0)
J-integral	Elastic-power law plastic	Small	Sharp (R=0)
Elastic compliance	Elastic	-	Sharp (R=0)
Unloading compliance	Elastic-power law plastic	Large	Blunt (R=0.003 mm)

In the present study, the commercial software package ADINA [7] was used. The use of large deformation in the present study for unloading compliance evaluation is to take the effect of ligament deformation on compliance into consideration; the blunt notch is to ensure convergence in the large-deformation analysis. Two-D nine-node isoparametric displacement-based plane strain elements with 3×3 integration were used for analysis of the clamped SE(T) specimens. The effect of 3-D and 3-D with side-grooves was also studied by FEA. Calculations conducted in the present study showed good convergence. For simulation of clamped SE(T) specimens, a rigid link was assumed between the loading point and two clamped surfaces on the SE(T) specimens. Figure 6, Figure 7, and Figure 8 show the finite element meshes for the clamped SE(T) specimen in 2-D, 3-D and 3-D with side-grooves. Detail of the mesh at the crack tip is also shown in the figure.

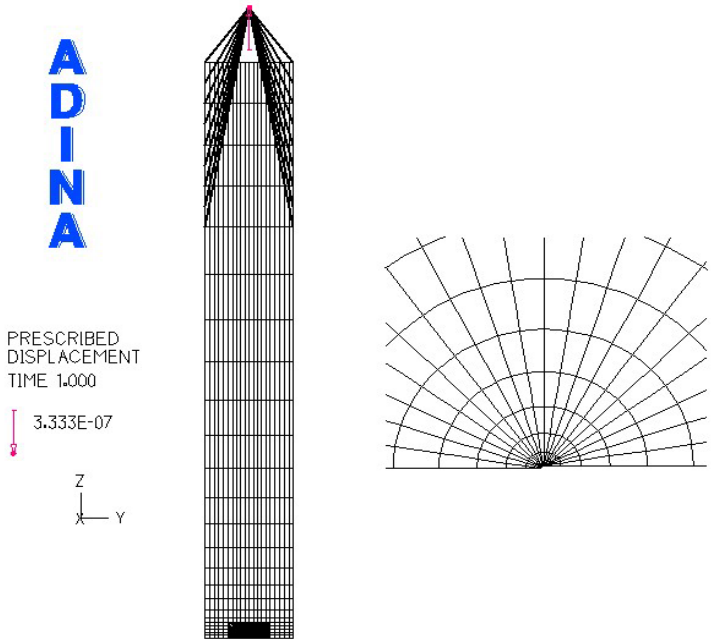

Figure 6. 2-D FEA mesh for clamped SE(T) specimen.

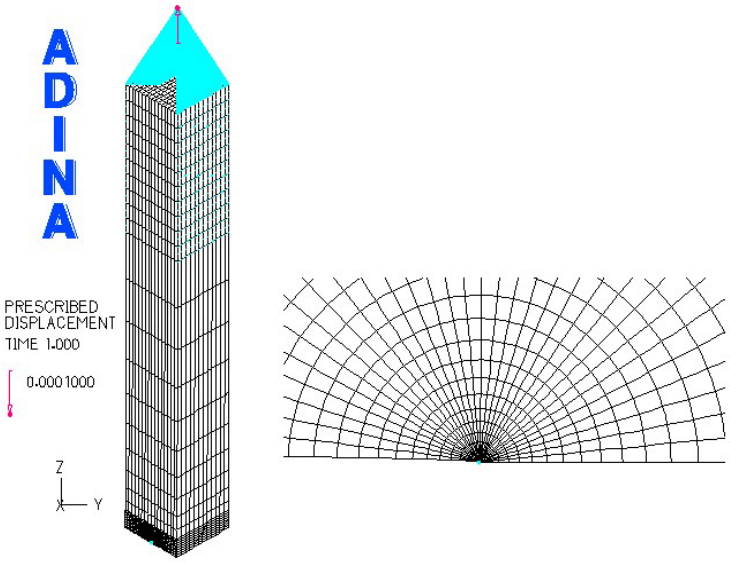

Figure 7. 3-D FEA mesh for clamped SE(T) specimen.

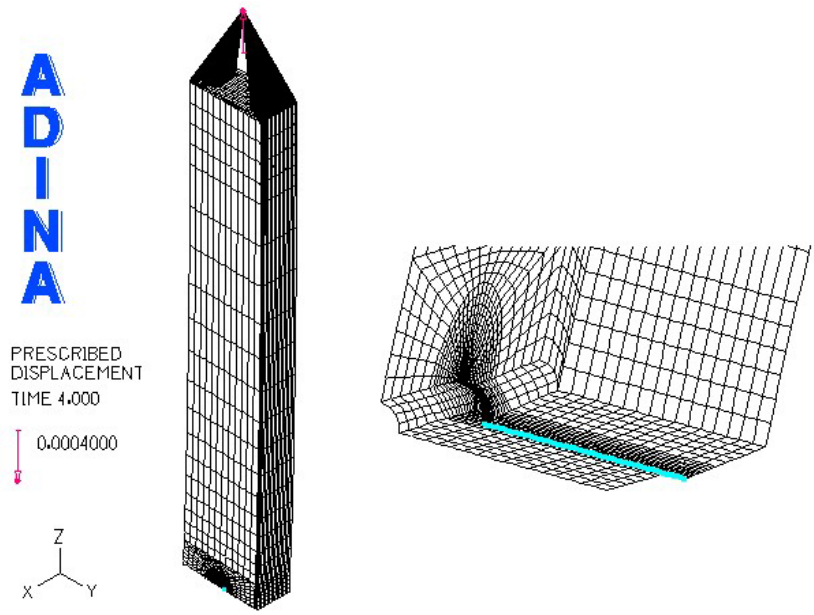

Figure 8. 3-D FEA mesh for clamped SE(T) specimen with side-groove.

3.3 EQUATIONS FOR STRESS INTENSITY FACTORS

Although the clamped SE(T) specimen is under displacement controlled loading, for convenient use, the stress intensity factor expression of this crack geometry is written as a function of the applied nominal stress instead of applied displacement:

$$K_{(i)} = \left[\frac{P_i \sqrt{\pi a_i}}{(BB_N)^{1/2} W} \right] G\left(\frac{a_i}{W}\right) \tag{5}$$

FEA was used to calculate the geometry factor in Eqn. (5) with H/W=10 and 0.05 ≤a/W≤0.95. The stress intensity factor in Eqn. (5) was converted from the J-integral using the following equation:

$$K_{(i)} = \sqrt{\frac{J_{(i)} E}{1-\nu^2}} \tag{6}$$

The J-integral was evaluated by the virtual crack extension (VCE) technique. The calculated G as a function of crack depth a/W was then fitted to the following polynomial by the least-squares technique:

$$G\left(\frac{a}{W}\right) = \sum_{i=1}^{12} t_i \left(\frac{a}{W}\right)^{i-1} \tag{7}$$

and the parameters t_i (i=1 to 12) are listed in Table 2.

Table 2. Coefficients t_i in Eqn. (7) for H/W=10 and 0.05≤a/W≤0.95

i	1	2	3	4	5	6	7	8
t_i	1.197	-2.133	23.886	-69.051	100.462	-41.397	-36.137	51.215
i	9	10	11	12				
t_i	-6.607	-52.322	18.574	19.465				

Figure 9 shows the comparison of the geometry factors from Eqn. (7) and that calculated by Ahmad et al [8] also recommended by DNV-RP-F108 [3].

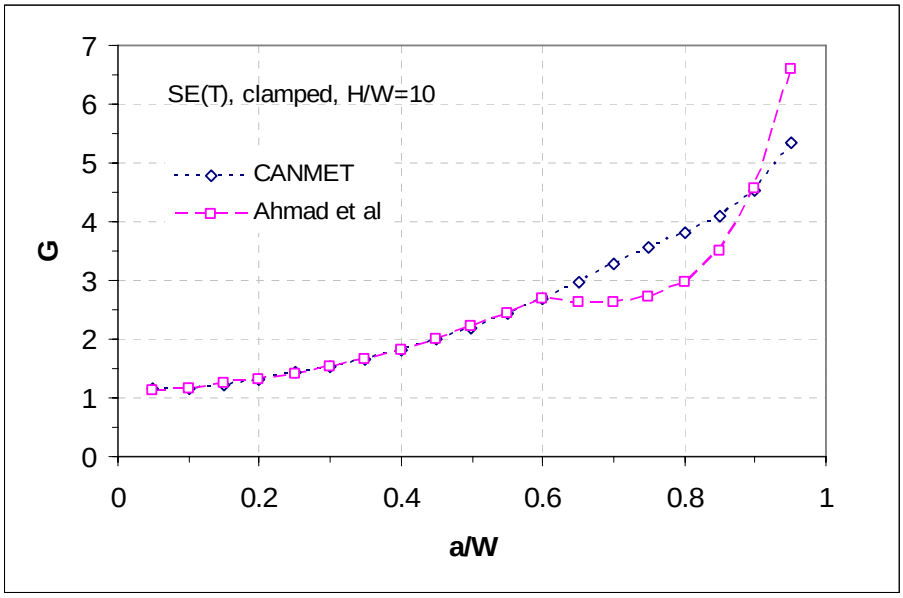

Figure 9. Geometry factor G for clamped SE(T) specimen, H/W=10.

It is seen that the results from CANMET and Ahmad et al [8] (also by DNV-RP-F108 [3]) agree well for 0.05≤a/W≤0.6 and an inconsistent kink occurs on the solution of Ahmad et al for a/W>0.6.

3.4 EQUATIONS FOR ELASTIC CMOD COMPLIANCE

When a single-specimen technique is used for J-resistance testing, the crack length is evaluated at closely spaced intervals during the test. The crack depth is conveniently evaluated using the measured crack mouth opening displacement (CMOD) compliance, such as that done in ASTM E1820 [5]. In the present study, the finite element technique was used to calculate the elastic CMOD compliance for clamped SE(T) specimens with H/W=10 and 0.05≤a/W≤0.95. The calculated elastic CMOD compliances, C (=$CMOD_e/(\sigma WB)$) written in normalized form (BCE′, where E′=E for plane stress and =$E/(1-\upsilon^2)$ for plane strain) and U (=$1/((BCE')^{1/2}+1)$) are listed in Table 3.

Table 3. CMOD compliance for SE(T) specimen, H/W=10.

a/W	0.050	0.100	0.200	0.300	0.400	0.500	0.600	0.700	0.800	0.900	0.950
BCE'	0.295	0.613	1.401	2.554	4.349	7.232	11.907	19.390	30.765	46.421	56.106
U	0.648	0.561	0.458	0.385	0.324	0.271	0.225	0.185	0.153	0.128	0.118

The calculated results were then fitted to the following equation for evaluating crack depth from the measured elastic CMOD compliance:

$$a/W = \sum_{i=0}^{9} r_i U^i \tag{8}$$

where

$$U_i = \frac{1}{\sqrt{BC_i E'} + 1} \tag{9}$$

The values of r_i are listed in Table 4.

Table 4. Coefficients r_j in Eqn. (10) for H/W= 10

j	0	1	2	3	4	5	6	7	8	9
r_j	2.044	-15.732	73.238	-182.898	175.653	60.930	-113.997	-113.031	8.548	142.840

Figure 10 shows the CMOD compliance as a function of a/W both for clamped SE(T) (H/W=10) specimens calculated by Eqn. 8 and for SE(B) specimens given by E1820. It is seen that a/W is very sensitive to the change of BCE for clamped SE(T) specimens. As a result, highly accurate CMOD compliance measurement is needed for clamped SE(T) specimens.

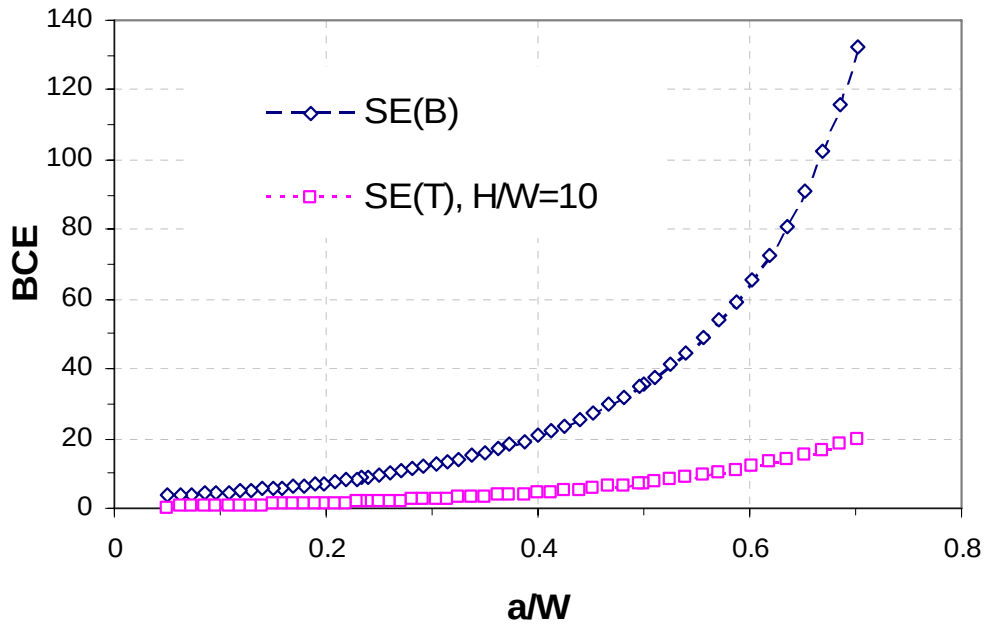

Figure 10. BCE vs a/W for clamped SE(T) and SE(B) specimens (plane stress).

In development of the compliance equation for crack evaluation, a 2-D FEA technique was used. Plane stress compliance equations are used for crack depth evaluation for SE(B) specimens in recent editions of ASTM E1820. In fact, the laboratory specimens are three-dimensional. Consequently, it is necessary to establish whether the plane stress assumption in the compliance equation (by using BCE in Eqn. (9)) is adequate. To do this, one 3-D B×B SE(T) specimen (H/W=10, a/W=0.5) was studied using FEA. The CMOD compliance calculated by FEA was used to evaluate the crack depth using Eqns. (8) and (9) with E'=E. The difference between the evaluated crack length and that of the FEA model was about 2%.

In ASTM E1820, side-grooving is recommended in J-resistance tests for SE(B) specimens to ensure a straight crack front; a total thickness reduction of 0.20 B is recommended. Any included angle of side groove less than 90° is allowed. Root radius shall be 0.5 ±0.2 mm. When side grooves are used, the thickness B is replaced by an effective thickness B_e using the following equation:

$$B_e = B - \frac{(B - B_N)^2}{B} \qquad (10)$$

where B_N=net thickness of the specimen.

To ensure a straight crack front for SE(T) specimen in J-resistance tests and reduce stress concentration at the side-groove, a similar shape but shallower side groove was selected. A side groove depth of 5% of the thickness on each side was used initially. Subsequent tests have indicated that 7.5% on each side might be more appropriate to ensure plane strain conditions. To show if Eqn. (10) works for SE(T) specimens in crack depth evaluation when side grooves are used, FEA was used to calculate the CMOD compliance of a side-grooved SE(T) specimen (H/W=10, a/W=0.5). Then the crack length was calculated using Eqns. (8) and (9) with the calculated compliance and effective thickness from Eqn. (10). It was found that the difference of

the calculated crack depth from Eqns. (8), (9) and (10) and that of the FEA model was about 1%. Figure 11 shows the calculated CMOD compliance for a 3-D crack and 3-D crack with 10% side-groove and that from 2-D equations (Eqns. (8) and (9) and (10)). It is seen that the compliance equations developed by the 2-D plane stress model can be used for 3-D SE(T) specimens (with or without side-grooves) with reasonable accuracy.

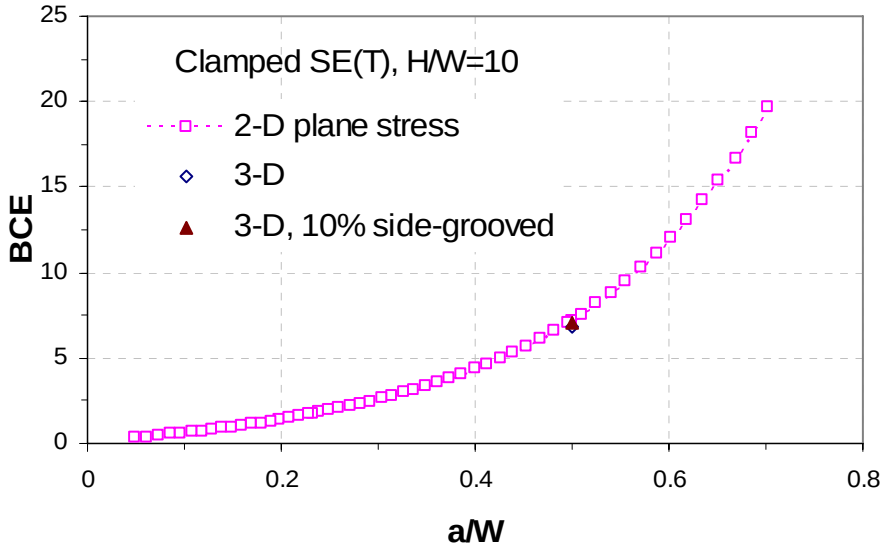

Figure 11. CMOD compliance from 3-D FEA and 2-D equations.

3.5 ROTATION CORRECTION FOR UNLOADING COMPLIANCE OF CLAMPED SE(T) SPECIMENS

The above elastic CMOD compliance equation (Eqn. 8) cannot be directly used for crack length evaluation for tension specimens, such as SE(T) [9, 10] because the specimen rotates so that the centre of the remaining ligament moves toward the load line. For this reason, correction for rotation is required when the unloading compliance technique is used on these specimens. The measured unloading compliance is modified in order to use in Eqn. (8) for crack depth evaluations:

$$C_{c(i)} = \frac{C_{(i)}}{F_r} \tag{11}$$

where C_i and $C_{c(i)}$ are the measured CMOD compliance at the i_{th} unloading, and compliance in the undeformed configuration, respectively. F_r is the rotation correction factor.

Rotation correction for clamped SE(T) specimens was assessed using FEA. The details are described in a separate publication [11].

In the FEA [11], it was found that:

1. The rotation correction coefficients of clamped SE(T) specimens are generally much smaller than those of pin-loaded SE(T) specimens with the same crack depth.
2. The effect of strain hardening on the rotation correction coefficients is small for $P/P_Y \leq 1.2$.

3. The rotation correction coefficients increase with increasing load. There is an approximately linear relationship between F_r and P/P_Y for clamped SE(T) specimens for $P/P_Y \leq 1.2$.
4. The rotation correction coefficients increase with increasing H/W and a/W.

Based on the above observations, an equation was developed to fit the results of FEA for rotation correction coefficients of clamped SE(T) specimens with H/W=10. In this equation, the rotation correction coefficients are dependent on load and crack depth [11]:

$$F_{r(i)} = \frac{1}{1 - 0.165 \frac{a_o}{W} \left(\frac{P_{(i)}}{P_Y} \right)} \tag{12}$$

Figure 12 and Figure 13 show the rotation factors calculated by FEA and Eqn. (12) for clamped SE(T) specimens (H/W=10) with deep and shallow cracks.

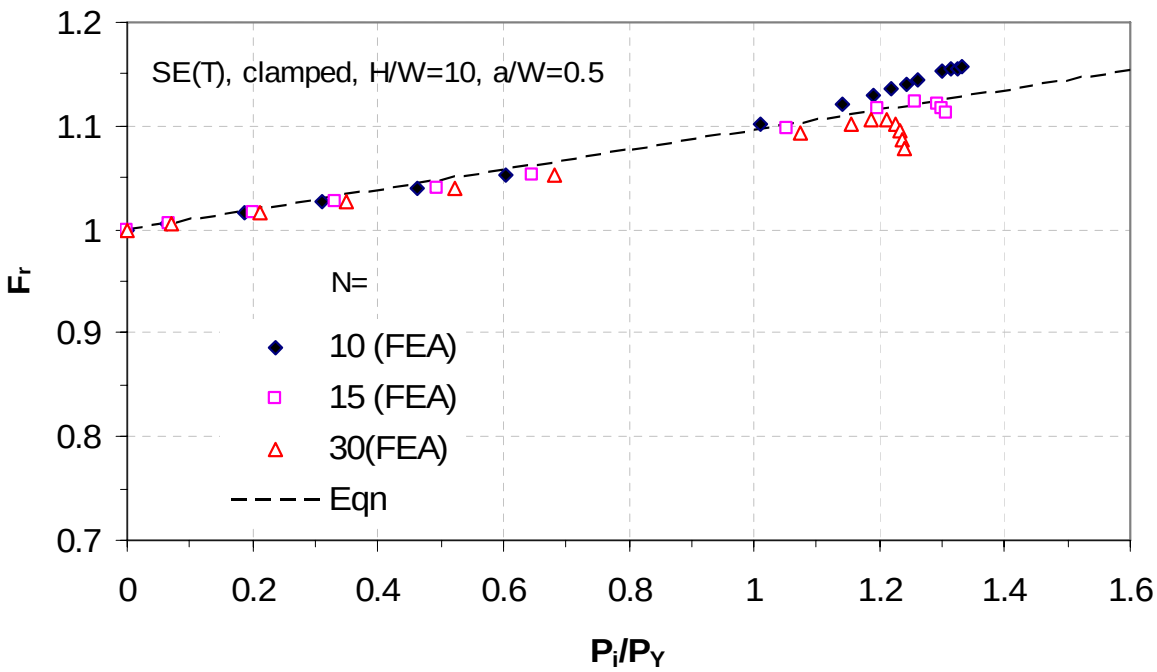

Figure 12. Rotation correction coefficients as functions of load for clamped SE(T) specimens (a/W=0.5).

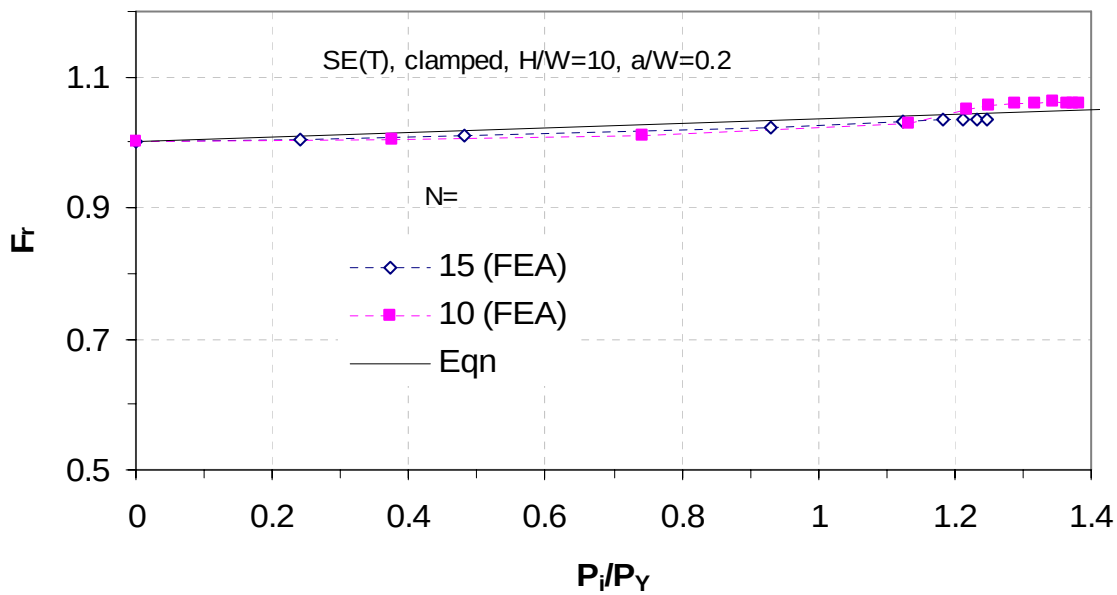

Figure 13. Rotation correction coefficients as functions of load for clamped SE(T) specimens (a/W=0.2).

3.6 EVALUATION OF FACTOR η_{CMOD}

Without considering crack growth, the plastic J-integral in Eqn. (3) can be written as:

$$J_{pl(i)} = \frac{\eta_{CMOD}}{Bb} A_{plCMOD(i)} \tag{13}$$

This equation can be used for evaluation of η_{CMOD} by employing FEA. To do this, FEA was conducted on clamped SE(T) specimens with H/W=10, a/W= 0.05, 0.1, 0.2, 0.3, 0.4, 0.5, 0.6 and 0.7. The factor η_{CMOD} can be found from the slope of a $J_{p(i)}$, $A_{plCMOD(i)}$/ Bb straight line evaluated from FEA. Figure 14 and Figure 15 show these straight lines for deep and shallow cracks, respectively.

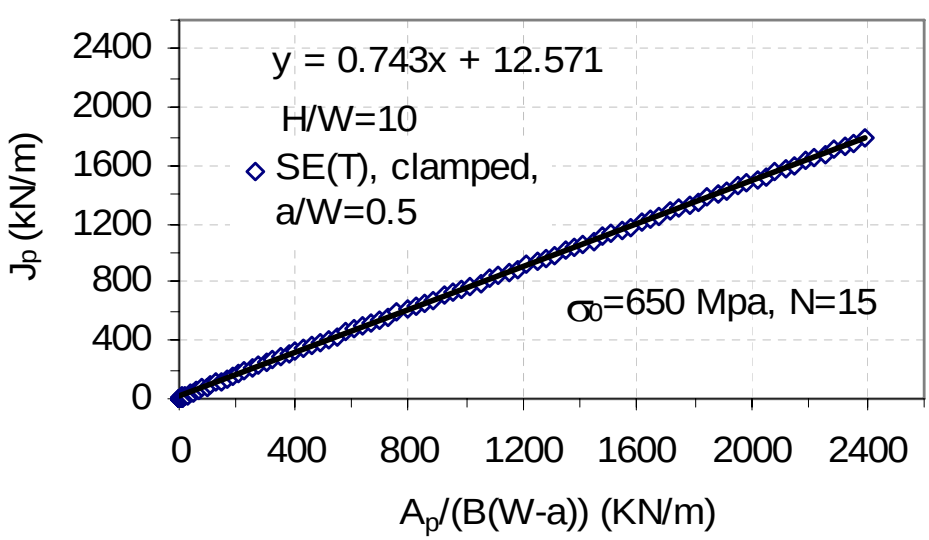

Figure 14. Slope of straight line $J_{P(I)}$, $A_{PLCMOD(I)}$/ Bb for deep crack (a/W=0.5).

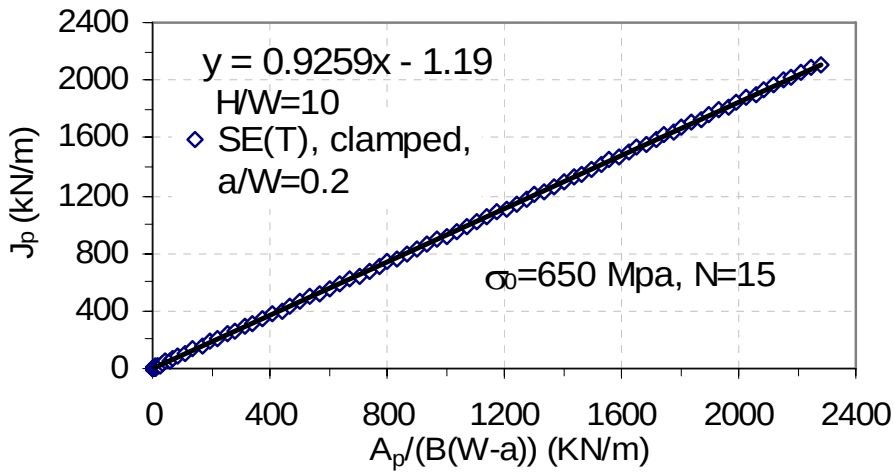

Figure 15. Slope of straight line $J_{P(I)}$, $A_{PLCMOD(I)}$/ Bb for shallow crack (a/W=0.2).

Figure 16 shows the parameters as a function of crack depth (a/W) for four material strain hardening exponents N=5, 10, 15 and 20.

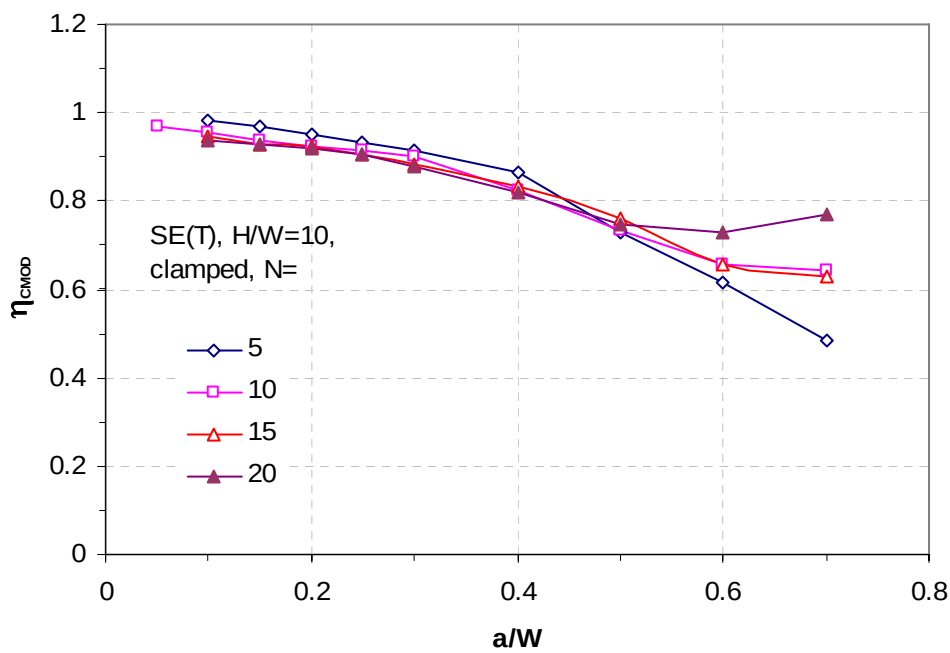

Figure 16. Parameter η_{CMOD} as a function of a/W for various N.

It is seen that η_{CMOD} is insensitive to material strain hardening exponent (N) for a/W≤0.5. This is consistent with results of Kirk and Dodds [12] for SE(B) specimens.

The data in Figure 16 were then fitted to a polynomial by the least squares technique (for a/W=0.7, only the data for N=10 and 15 were used in the fit):

$$\eta_{CMOD} = \sum_{i=0}^{10} \phi_i (a/W)^i \qquad (14)$$

The coefficients ϕ_i are listed in Table 5.

Table 5. Coefficients ϕ_i in Eqn. (5)

i	0	1	2	3	4	5	6	7	8
ϕ_i	1.000	-1.089	9.519	-48.572	109.225	-73.116	-77.984	38.487	101.401
i	9	10							
ϕ_i	43.306	-110.770							

Figure 17 shows compares the parameter η_{CMOD} calculated using Eqn. 14 with that proposed in DNV-RP-F108 [3] for B/W=5 and Cravero and Ruggieri [10]. Generally speaking, these three solutions agree well.

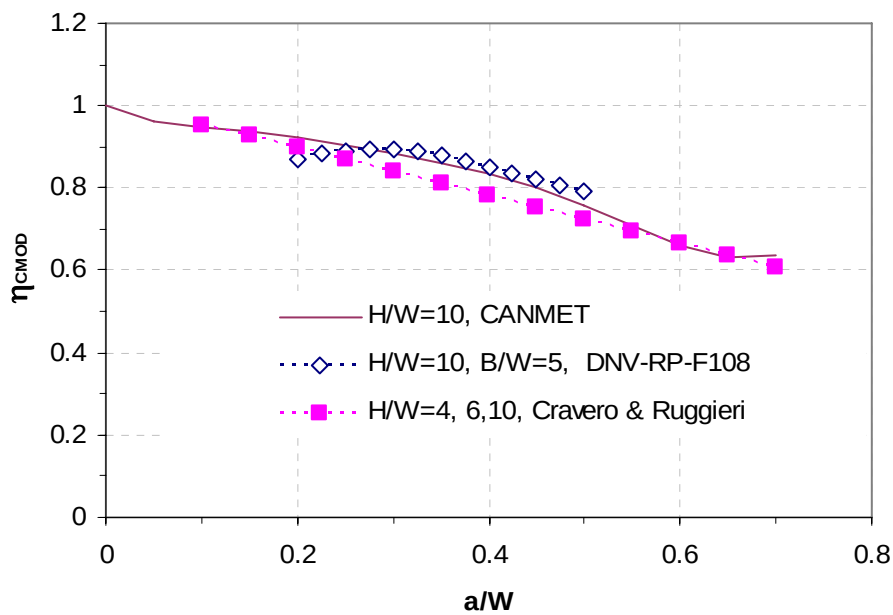

Figure 17. Comparison of ηCMOD factors.

3.7 J EVALUATION FOR GROWING CRACK

For a growing crack, J estimation should consider a crack growth correction as shown in Eqn. 3 where a factor of γ_{LLD} is used, as suggested by Zhu et al [13].

According to Ernst et al [14], γ_{LLD} can be calculated from η_{LLD} using the following equation:

$$\gamma_{LLD} = \eta_{LLD} - 1 - \frac{b_i}{W}\frac{\eta_{LLD}'}{\eta_{LLD}} \qquad (15)$$

Figure 18 shows η_{LLD} as function of a/W for clamped SE(T) specimens (H/W=10) calculated by FEA for materials with strain hardening exponent N=15 and 20.

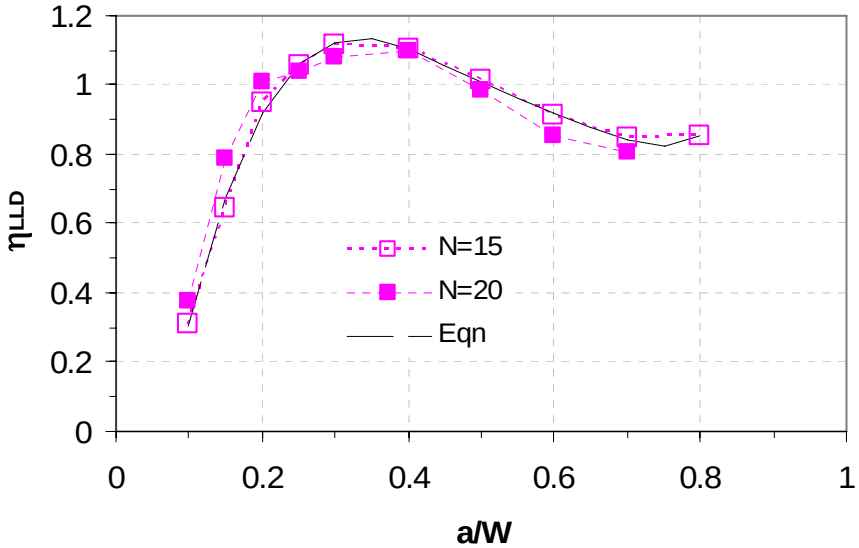

Figure 18. Factor η_{LLD} as a function of a/W for clamped SE(T) specimens, H/W=10.

The calculated η_{LLD} as function of a/W for clamped SE(T) specimens (H/W=10) was then fitted to a polynomial by the least squares technique:

$$\eta_{LLD} = \sum_{i=0}^{10} \psi_i (a/W)^i \tag{16}$$

The coefficients ψ_i were listed in Table 6.

Table 6. Coefficients ψ_i in Eqn. (16) for H/W=10 and 0.1≤a/W≤0.7

i	0	1	2	3	4	5	6	7	8
ψ_i	-0.880	15.190	-35.440	18.644	18.399	-1.273	-12.756	-12.202	-4.447
i	9	10							
ψ_i	5.397	14.187							

Substituting Eqn. (16) into Eqn. (15), γ_{LLD} can be calculated. For use in Eqn. (15), η'_{LLD} is written as:

$$\eta'_{LLD} = \sum_{i=1}^{10} i\psi_i (a/W)^{i-1} \tag{17}$$

Figure 19 shows the calculated γ_{LLD} as a function of a/W.

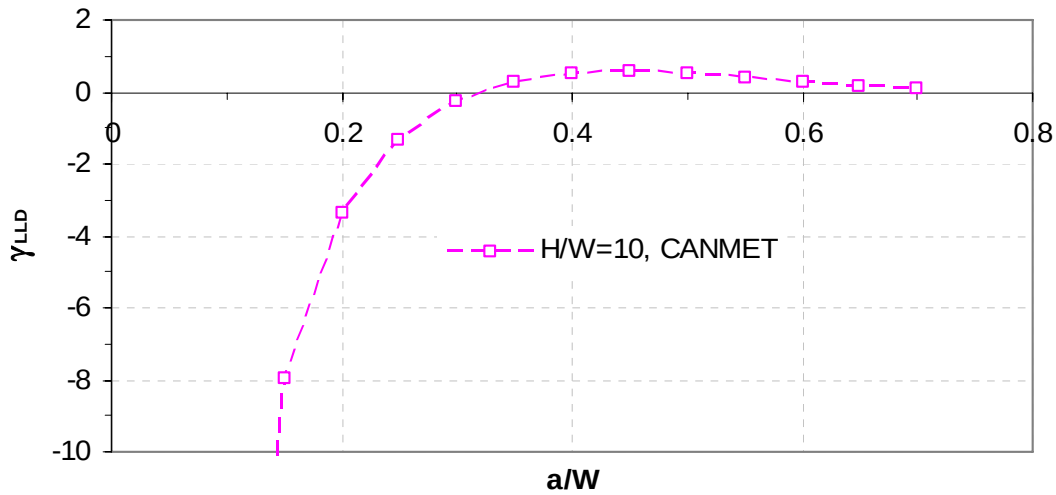

Figure 19. γ_{LLD} as a function of a/W.

4 EXPERIMENTS

J-resistance tests using the single specimen technique on clamped SE(T) specimens were conducted in the present study following the procedure developed in the above sections. The equations developed in the above section for J-integral and for crack length evaluations using an unloading compliance technique with rotation correction were used. For comparison, J-resistance tests using SE(B) specimens with shallow and deep cracks were also conducted. The latter tests were conducted according to ASTM E 1820.

4.1 MATERIALS AND SPECIMENS

The material used in the present study was cut from 1219 mm diameter, 14.3 mm wall thickness X100 steel pipe. The tensile properties of the steel were measured using round specimens (8 mm diameter) oriented in the longitudinal direction of the pipe. Four specimens were tested and the measured tensile properties are listed in Table 7.

Table 7. Tensile properties

Specimen #	Diameter (mm)	YS (0.2%) MPa	YS (0.5%) MPa	UTS MPa	El (%)	RA (%)
A1	8.01	667	630	806	21.2	51.6
A2	8.00	663	630	808	21.4	52.1
A3	8.00	695	654	824	21.0	46.5
A4	8.00	696	662	817	20.8	53.3
Avg	8.00	680	644	814	21.1	50.9

The stress-strain curves of these four specimens are shown in Figure 20. It can be seen that all curves exhibit continuous yielding behavior and have a uniform strain close to 5%.

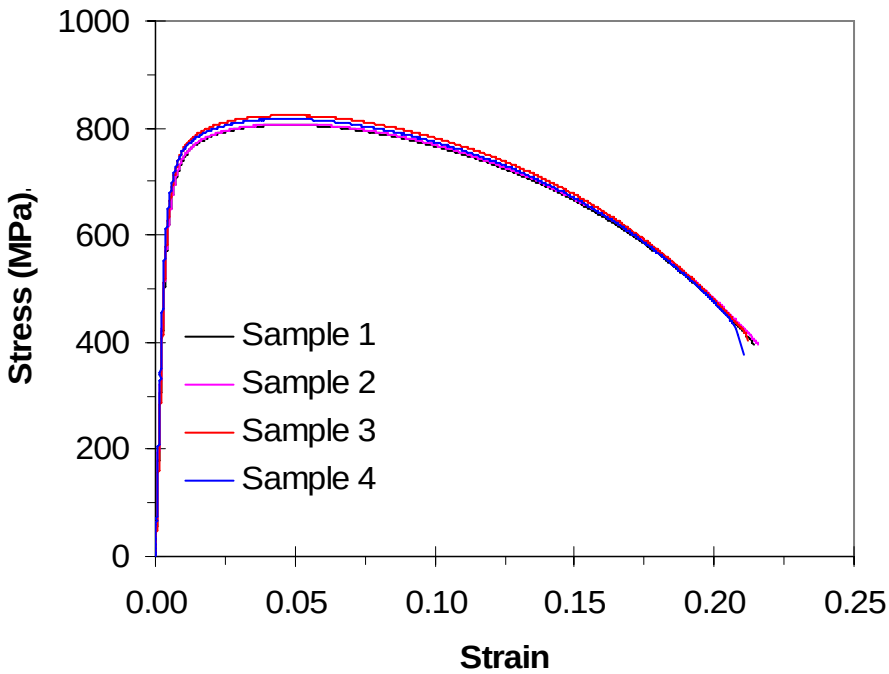

Figure 20. Stress-strain curves of X100 steel pipe in longitudinal direction (parallel to the pipe axis).

The SE(T) and SE(B) specimens were taken from the X100 pipe steel with a crack plane orientation L-R (ASTM E1823 [15]). B×B specimens were used with B (=12.7 mm) close to the wall thickness of the pipe. The target crack length was 6.35 mm (a/W=0.5) for a deep crack and 3.175 mm (a/W=0.25) for a shallow crack. For each crack length (either SE(T) or SE(B)), six specimens were prepared with three of them side-grooved. The shape of the side-grooves was inadvertently machined to smaller radius (r=0.15 mm) than suggested in ASTM E1820-06 (r=0.3-0.7 mm). The depth of the side-groove was 10% at each side for SE(B) and 5% at each side for SE(T) specimens. The span length of the SE(T) specimens is 127 mm (H/W=10) with an additional 50 mm (≈4W) at each end for gripping. All specimens were fatigue precracked following the procedure described in E1820-06 for SE(B) or the procedure described above for SE(T) specimens.

4.2 J-R TESTS USING CLAMPED SE(T) SPECIMENS

Following the procedure described in Section 2, load-CMOD curves with about 35 to 50 load-unload sequences were measured for clamped SE(T) specimens. Figure 21 shows the P-CMOD curves for two clamped SE(T) specimens (one with a deep crack a/W=0.5 and one with a shallow crack a/W=0.25). Figure 22 shows the unloading compliance (BCE) changes as a function of unloading number during loading in the J-R tests. It is seen that the compliance continually increases with loading in which crack growth occurs. However, there is a compliance decrease before maximum load where rotation reduces the unloading compliance, especially for a/W=0.5 where rotation reduce the compliance to about 8% at maximum load. The unloading compliance was then used to evaluate the crack length with rotation considered by using Eqn. (12). The evaluated crack length and the load/plastic CMOD curve was then used to evaluate the

J-integral using Eqn. 3. Figure 23 and Figure 24 show the resultant J-R curves for six SE(T) specimens with a/W=0.5 (3 plain-sided and 3 side-grooved) with and without rotation correction on unloading compliance respectively. In Figure 24, the a_{oq} adjustment recommended in ASTM E1820-06 was applied to the data after rotation correction. The adjustment was small (less than 0.06 mm). The curves for plain-sided specimens lie slightly above those for side-grooved specimens, although the difference is well within the scatter band. Figure 23 shows a pronounced "negative crack growth" that results from the use of uncorrected compliance values in Eqn. (8). Rotation correction according to Eqns. (11) and (12) remove this artefact and enables a useful resistance curve to be generated from each specimen. Figure 25 and Figure 26 show the resultant J-R curves for five SE(T) specimens with a/W=0.25 (two plain-sided and three side-grooved) with and without rotation correction on crack length respectively. Again, in Figure 26, the a_{oq} adjustment recommended in ASME E1820-06 was applied to the data after rotation correction. It is seen that the J-resistance curves in Figure 25 and Figure 26 are almost identical because the rotation correction is very small for shallow cracks. At the maximum load, the CMOD compliance correction is only about 3% and so has an insignificant effect on crack length.

Figure 27 shows the effect of factor γ on J-resistance curves for a deep (a/W=0.5) and a shallow (a/W=0.25) clamped SE(T) specimens. The curves with solid symbols are the J-R curves calculated using Eqn. (3) with γ=0 (i.e., no crack growth correction is considered in J-integral evaluation) while the curves with open symbols are the J-R curves calculated using Eqn. (3) with $\gamma = \gamma(a/W)$ (i.e., crack growth correction is considered in J-integral evaluation by using γ_{LLD} described in Eqn. (15)). It is seen that the difference is small (maximum difference ≈6%).

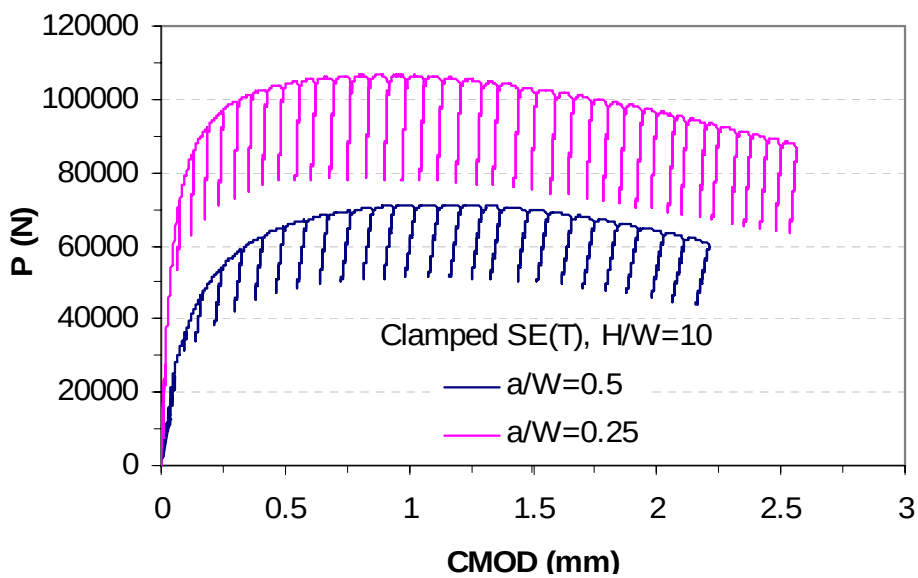

Figure 21. P-CMOD curves of clamped SE(T) specimens, X100 steel.

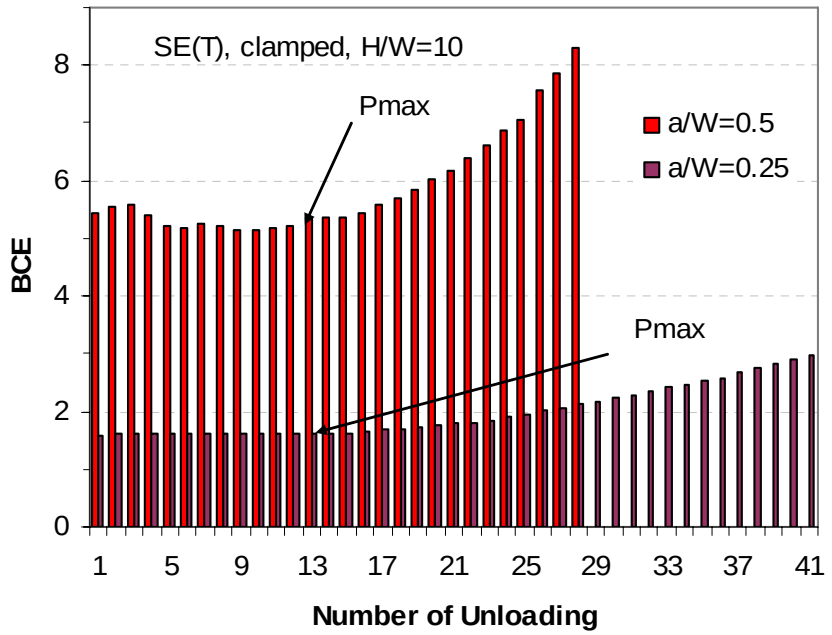

Figure 22. Change of unloading compliance during loading-unloading sequence.

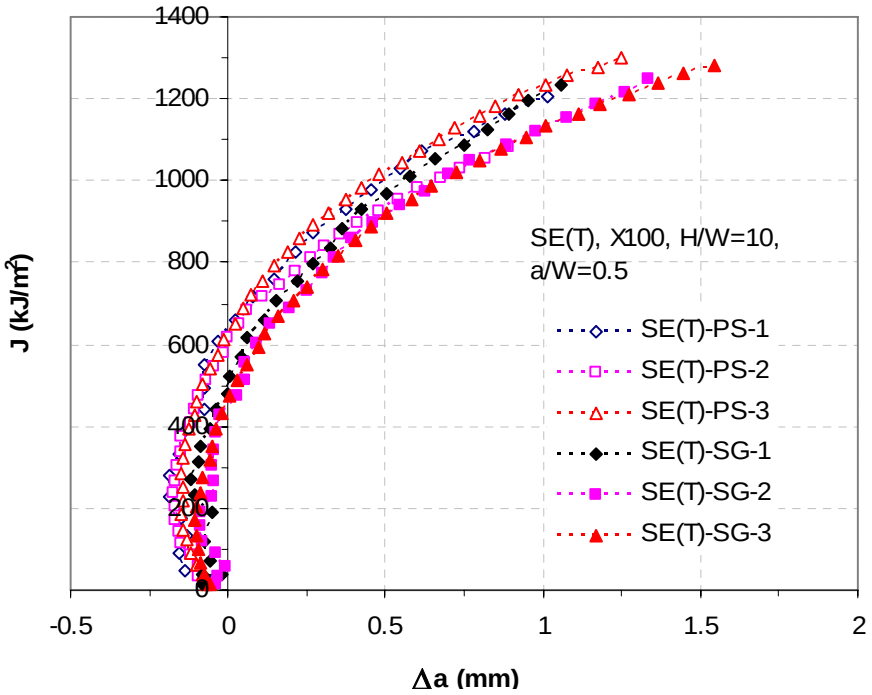

Figure 23. J-R curves for deeply-cracked SE(T) specimens, crack length without rotation correction (PS-plain-sided, SG-side-grooved).

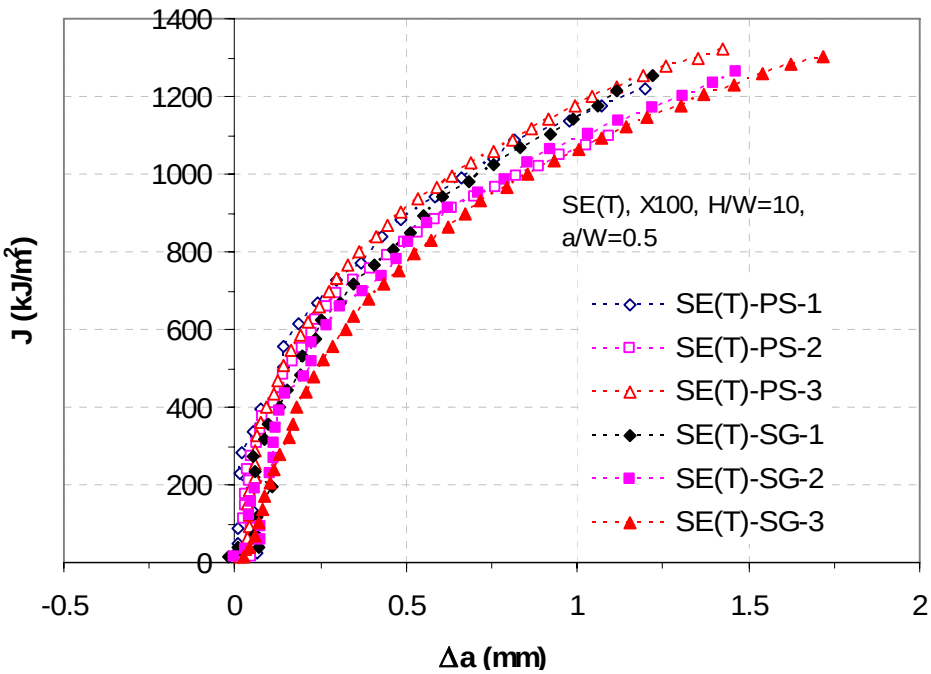

Figure 24. J-R curves for deeply-cracked SE(T) specimens, crack length with rotation correction (PS-plain-sided, SG-side-grooved).

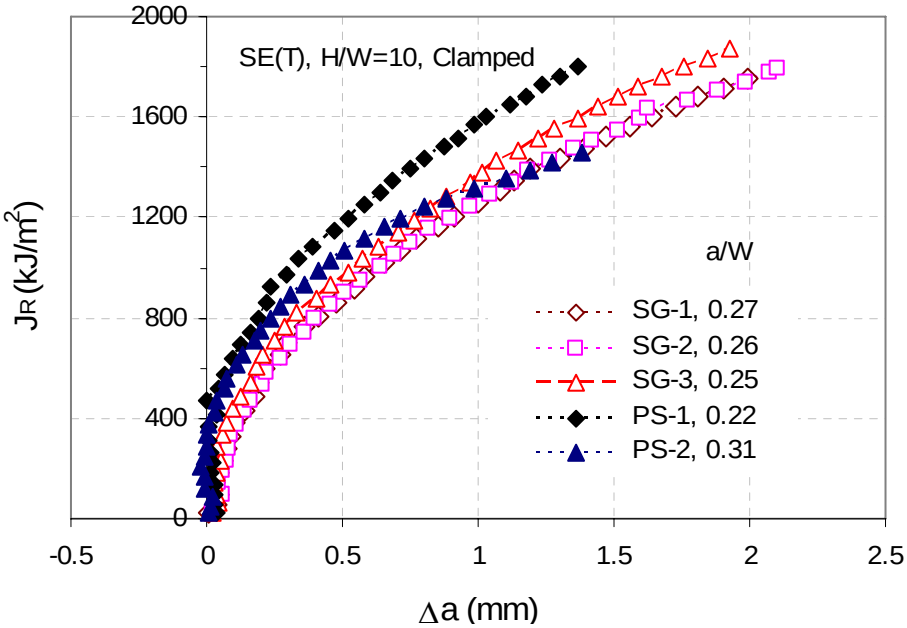

Figure 25. J-R curves for shallow-cracked SE(T) specimens, crack length without rotation correction (PS: plain-sided, SG: side-grooved).

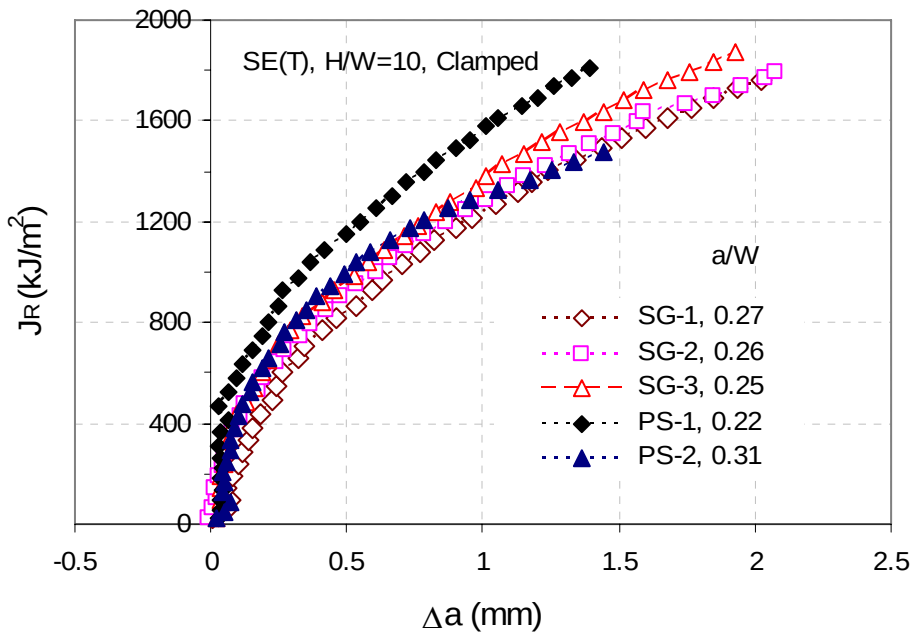

Figure 26. J-R curves for shallow-cracked SE(T) specimens, crack length with rotation correction (PS: plain-sided, SG: side-grooved)

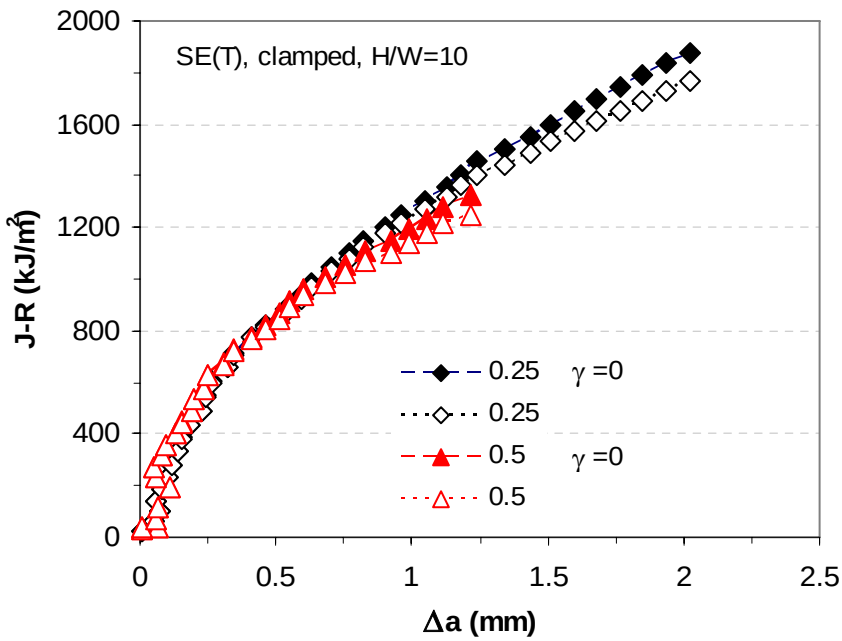

Figure 27. Effect of γ on J-Integral evaluation.

At the start of each test, CMOD compliance was measured to estimate the original crack length, a_o. Three unloading/reloading sequences in a load range from 0.5 to 1.0 P_f (P_f=0.5B_N(W-a)σ_y) were conducted. The average of the crack lengths evaluated in these three unloading/ reloading sequences was defined as initial crack length measured by compliance technique. After testing, the specimen was heat tinted at about 300°C for 30 min and then broken apart. The nine-point-average technique described in ASME E1820 was used to measure the crack length. The initial

and final crack lengths measured on the broken specimens were then compared with that from the compliance technique.

Figure 28 compares measured crack lengths and those from the compliance technique for eleven clamped SE(T) specimens (plain-sided and side-grooved, a/W=0.2-0.5). For the side-grooved specimens, the effective thickness B_e was estimated according to Eqn. (10) following E1820-06 [5]. It is seen that the agreement is excellent.

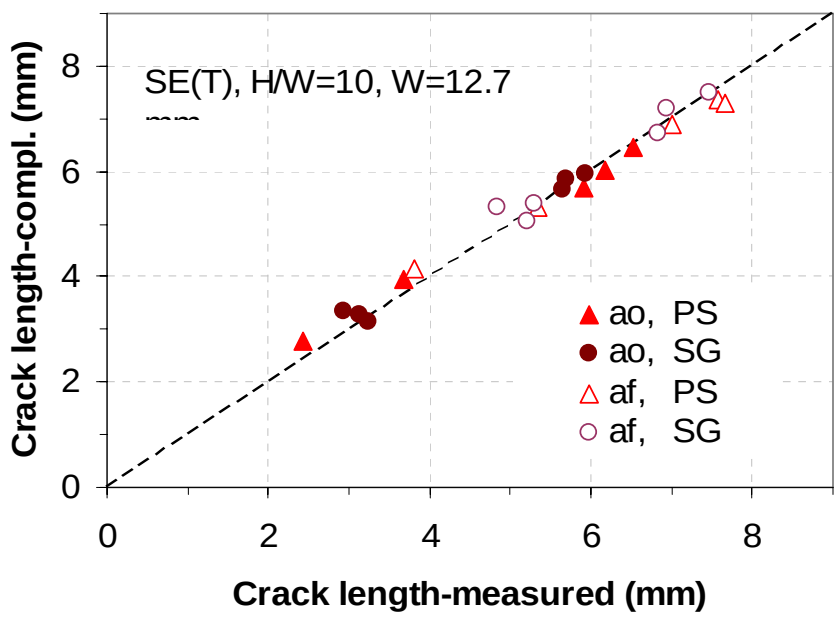

Figure 28. Crack length for clamped SE(T) specimens, a_o, a_f-initial and final crack lengths; PS, SG-plain sided and side-grooved specimens.

4.3 J-R TESTS USING SE(B) SPECIMENS

J-R tests on SE(B) specimens (B×B, B=12.7 mm) with deep (a/W=0.5) and shallow (a/W=0.25) cracks, including plain-sided and side-grooved specimens, were conducted on the same X100 steel pipe material with the cracks oriented in the through-thickness direction. All SE(B) tests were conducted following ASTM E1820-06 with some modification of factors η and γ for shallow cracks according to Zhu et al. [16]:

$$\eta = 0.397 + 8.966\left(\frac{a}{W}\right) - 12.495\left(\frac{a}{W}\right)^2 \qquad a/W < 0.397$$
$$\eta = 2 \qquad a/W \geq 0.397 \tag{18}$$

and

$$\gamma = -15.08 + 145.16\left(\frac{a}{W}\right) - 503.87\left(\frac{a}{W}\right)^2 + 639.61\left(\frac{a}{W}\right)^3 \qquad a/W < 0.397$$
$$\gamma = 1 \qquad a/W \geq 0.397 \tag{19}$$

Figure 29 and Figure 30 show the J-resistance curves measured using SE(B) specimens with deep (a/W=0.5) and shallow (a/W=0.25) cracks respectively.

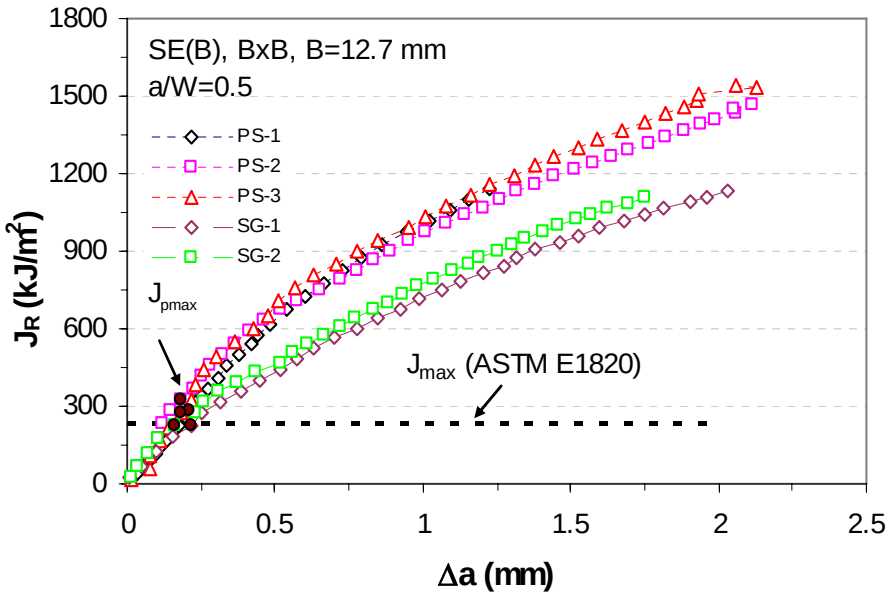

Figure 29. J-R curves for deeply-cracked (a/W=0.5) SE(B) specimens, PS: plain-sided, SG: side-grooved.

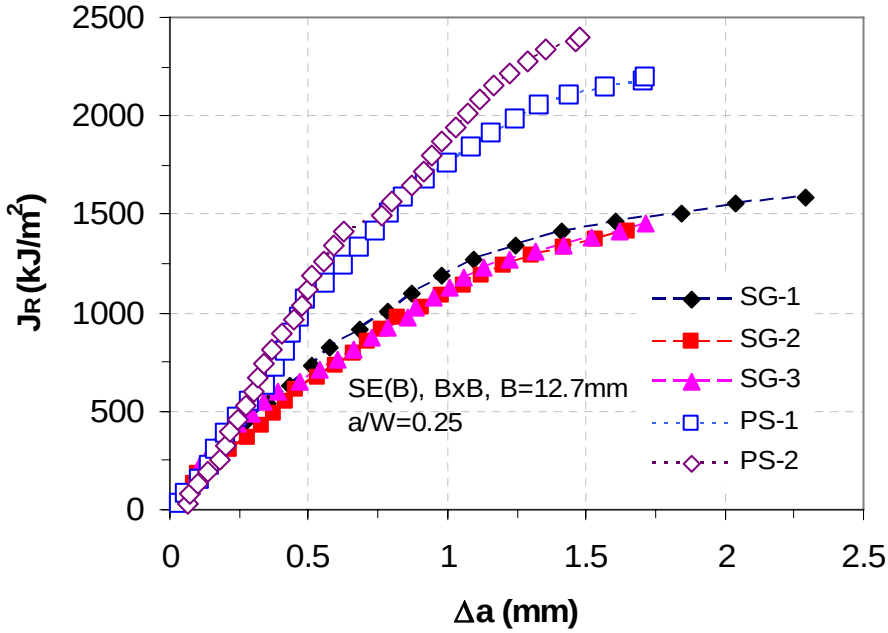

Figure 30. J-R curves for shallow-cracked (a/W=0.5) SE(B) specimens, PS: plain-sided, SG: side-grooved.

For a/W=0.5, the J-integral at maximum load, J_{pmax}, is also shown in the figure.

To ensure that SE(B) tests are in a situation of high constraint and size-independent, ASTM E1820 gives strict requirements on specimen size (B and b):

$$J_{\max} = \frac{b\sigma_Y}{20} \qquad or \qquad J_{\max} = \frac{B\sigma_Y}{20} \tag{20}$$

The calculated J_{max} is also shown in Figure 29. It is seen that most of the data on the J-R curves are larger than J_{max}. Obviously, a J-R curve that is valid according to ASTM E1820 cannot be measured using deeply-cracked SE(B) specimens with this thickness because most data will be beyond the J_{max} limit. However, although not size-independent, the results are still applicable to cracks of similar geometries, such as for assessment of cracks in pipe of the same thickness.

4.4 COMPARISON OF J-R CURVES MEASURED USING SE(T) AND SE(B) SPECIMENS

Figure 31 and Figure 32show the comparison of J-R curves measured by using SE(T) and SE(B) specimens, both for deep cracks (a/W=0.5) and shallow cracks (a/W=0.25), including plain-sided and side-grooved specimens, respectively.

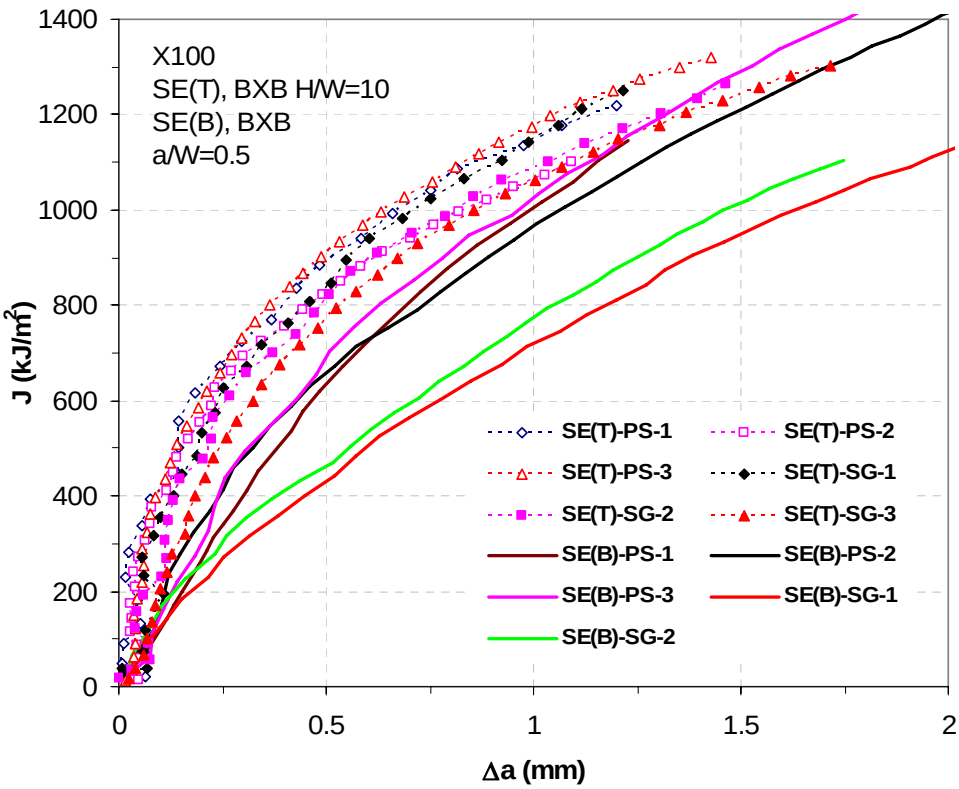

Figure 31. J-R curves measured using SE(T) and SE(B) specimens, a/W=0.5.

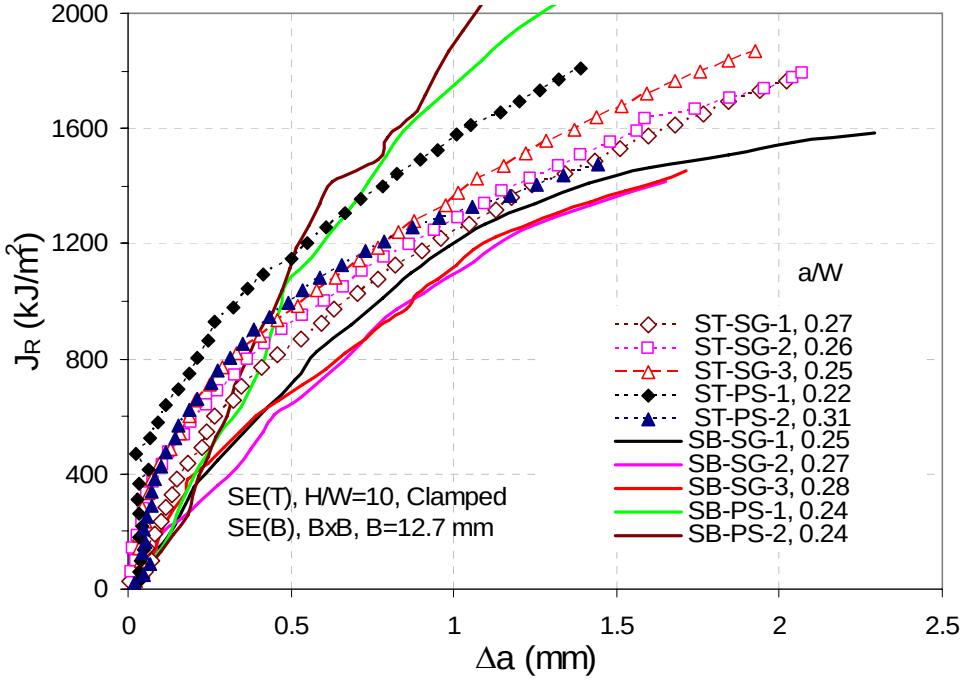

Figure 32. J-R curves measured using SE(T) and SE(B) specimens, a/W=0.25

For deep cracks, the J-R curves measured using clamped SE(T) specimens are higher than those using SE(B) specimens, especially when Δa≤0.5 mm. It is also seen that there is significant difference between the J-R curves of the plain-sided and side-grooved (10% at each side) SE(B) specimens while the difference is insignificant between the J-R curves of the plain-sided and side-grooved (5% at each side) SE(T) specimens. For shallow cracks, the J-R curves measured by using clamped SE(T) specimens are higher than those using SE(B) specimens when Δa≤0.4 mm. It can be concluded that both for shallow and deep cracks, the crack initiation resistance of clamped SE(T) specimens is higher than of SE(B) specimens.

5 SUMMARY AND CONCLUSIONS

In the present study, comparison of crack-tip stress fields and constraints have shown that the best constraint matching for surface circumferential cracks in pipe is found for clamped SE(T) specimens with H/W=10. A procedure similar to that of ASTM E1820-06 for single-edge bend (SE(B)) and compact tension (C(T)) specimens was developed to measure the J-integral resistance of clamped SE(T) specimens using a single-specimen technique. All the equations used in the procedure, including those for evaluation of J-integrals from the area under load/plastic crack mouth opening displacement (CMOD) curves, and evaluation of crack length from unloading compliance including rotation correction, were developed using finite element analysis (FEA) for crack depth a/W= 0.2 to 0.5. SE(T) specimens made of X100 pipe steel with deep (a/W=0.5) and shallow (a/W=0.25) cracks, including those with 5% side-grooves at each side were tested using the developed procedure. Comparisons were made of the J-resistance curves measured using clamped SE(T) specimens and SE(B) specimens with the same crack depth. The following conclusions can be drawn:

1) A procedure has been developed to measure low-constraint J-resistance in tension using clamped SE(T) specimens and a single-specimen technique with crack length measured by unloading compliance. The procedure has been successfully applied to measurement of J-R curves of a high-strength X100 steel pipe material with a through-thickness notch orientation.
2) Precautions and techniques for compliance measurement special to the SE(T) geometry are described in the procedure.
3) A side-groove depth of 5% thickness at each side was found to be satisfactory, although subsequent experiments to optimize side-groove geometry indicated that 7.5% of thickness might be more appropriate to generate plane strain conditions. The B_e formulae proposed in E1820-06 to estimate effective thickness of side-grooved SE(B) specimens also works for clamped SE(T) specimens.
4) An equation for evaluation of J-integrals using the area under the load-plastic CMOD curve for the SE(T) geometry similar to that proposed in E1820-06 for SE(B) specimens was developed using FEA.
5) The geometry factor G used for evaluation of the elastic J-integral (J_e) agrees well with that proposed by Ahmad et al [8] and DNV-RP-F108 [3] for $a/W \leq 0.6$. For $a/W > 0.6$, it was found that an inconsistent kink occurs in the solution of Ahmad et al.
6) The factor η_{CMOD} used in evaluation of the plastic J-integral J_p was evaluated by FEA and found to agree well with that proposed in DNV-RP-F108 [3].
7) Correction to J for crack growth using a factor γ for clamped SE(T) specimens was developed using FEA. It was found that the effect of crack growth on the J-integral evaluation is less than 6% for the clamped SE(T) specimen, steel pipe material, and extent of crack growth evaluated.
8) A CMOD compliance equation was developed to evaluate the crack length of clamped SE(T) specimens using unloading compliance. Comparing the compliance with that of SE(B) specimens, the crack length of clamped SE(T) specimens is much more sensitive to the unloading compliance. Thus more accurate compliance measurement is needed for crack length evaluation in a clamped SE(T) specimen.
9) For clamped SE(T) specimens, the effect of specimen rotation on the unloading compliance has to be considered in crack length evaluation. The rotation correction coefficients increase with increasing H/W and a/W but are insensitive to strain hardening exponent N for $P/P_Y \leq 1.2$. The rotation correction coefficients increase with increasing load. There is an approximately linear relationship between rotation coefficient F_r and P/P_Y for clamped SE(T) specimens for $P/P_Y \leq 1.2$. A simple equation is proposed to relate F_r to P/P_Y.
10) Crack lengths estimated from unloading compliance were compared with measured values for eleven clamped SE(T) specimens, both plain-sided and side-grooved, with $0.2 \leq a/W \leq 0.6$, with the effective thickness B_e given by Eqn. (10) for side-grooved specimens. The agreement was excellent.
11) J-R curves measured using SE(T) and SE(B) specimens were compared both for deep cracks ($a/W \approx 0.5$) and shallow cracks ($a/W \approx 0.25$). For deep cracks, the J-R curves measured using clamped SE(T) specimens were higher than those using SE(B) specimens, especially when $\Delta a \leq 0.5$ mm. For shallow cracks, the J-R curves measured using clamped SE(T) specimens were higher than those using SE(B) specimens for $a/W \leq 0.4$ mm.

6 ACKNOWLEDGMENTS

This work is part of a larger consolidated program jointly funded by the Canadian Federal Government Program of Energy Research and Development (PERD), the Pipeline and Hazardous Materials Safety Administration of the U.S. Department of Transportation (DOT), and the Pipeline Research Council International, Inc. (PRCI). The views and conclusions in this paper are those of the authors and should not be interpreted as representing the official policies of any of these organizations.

7 REFERENCES

[1] ASTM E 1290-02, Standard Test Method for Crack-Tip Opening Displacement (CTOD) Fracture Toughness Measurement, ASTM International, West Conshohocken, USA

[2] Shen, G., Tyson, W. R., Glover, A. and Horsley, D., "Constraint Effects on Linepipe Toughness", 4th Int. Conference on Pipeline Technology, Scientific Surveys Limited, Ostend, Belgium, May, 2004.

[3] Recommended Practice DNV-RP-F108, "Fracture Control for Pipeline Installation Methods Introducing Cyclic Plastic Strain", Det Norske Veritas, 2006.

[4] Silva, A. L., Cravero, S. and Ruggieri, C., "Correlation of fracture behavior in high pressure pipelines with axial flaws using constraint designed test specimens". Part II: 3-D effects on constraint", Eng. Fracture Mechanic*s*, 73, pp. 2123-2138; 2006.

[5] ASTM E 1820-06, Standard Test Method for Measurement of Fracture Toughness, ASTM International, West Conshohocken, USA

[6] Shen, G., Bouchard, R., Gianetto, J.A. and Tyson, W.R., "Fracture Toughness Evaluation of High Strength Steel Pipe", Proceedings of PVP2008, ASME Pressure Vessel and Piping Division Conference, Chicago, Illinois, USA, July 27-31, 2008.

[7] ADINA, "Theory and Modeling Guide", Volume 1, Report ARD 01-7, ADINA R&D Inc, Watertown, USA, 2001.

[8] Ahmad, J., Papaspyropoulos, V. and Hopper, A. T., "Elastic-plastic analysis of edge-notched panels subjected to fixed grip loading," Eng. Fracture Mechanics, Vol. 38, 283-294; 1991.

[9] Joyce J.A. and Link R.E., "Effect of Constraint on Upper Shelf Fracture Toughness". Fracture Mechanics, 26th Volume, ASTM STP 1256, Walter G. Reuter, John H. Underwood and James C. Newman, Jr., Eds., ASTM, Philadelphia, pp. 142-177; 1995.

[10] Cravero S. and Ruggieri C. "Estimation Procedure of J-resistance Curves for SE(T) Fracture Specimens Using Unloading Compliance". Eng. Fracture Mechanics, Vol. 74, pp. 2735-2757; 2007

[11] Shen, G. and Tyson, W.R., "Crack Length Evaluation for SE(T) Testing Using Unloading Compliance in Single-Specimen Single-Edge-Notched Tension Fracture Toughness Testing", Journal of Testing and Evaluation, JTE102368, Vol. 37, No.4, 347-357; 2009.

[12] Mark T. Kirk and Robert H. Dodds. Jr., "J and CTOD Estimation Equations for Shallow Cracks in Single Edge Notch Bend Specimens", Journal of Testing and Evaluation, JTEVA, Vol. 21, 228-238; 1993.

[13] Xian-Kui Zhu, Brian N. Leis, and James A. Joyce, "Experimental Estimation of J-R Curves from Load-CMOD Record for SE(B) Specimens", Journal of ASTM International, Vol. 5, No. 5, Paper ID JAI101532, 2008.

[14] Ernst, H. A., Paris, P. C., and Landes, J. D., "Estimations on J-integral and Tearing Modulus T from a Single Specimen Test Record," Fracture Mechanics: 13th Conference, ASTM STP 743, ASTM International, West Conshohocken, PA, pp. 476–502, 1981.

[15] ASTM E 1823-96, "Standard Terminology Relating to Fatigue and Fracture Testing", ASTM, West Conshohocken, PA, USA.

[16] Zhu, X. K., Leis, B. N., Shen, G. and Tyson, W.R. "Experimental Determination of Constraint Dependent J-R Curves for X80 Pipeline Steel Using Normalization Method", Proceedings of IMECE2006, IMEC2006-13180, Chicago, USA, November 2006.